Energy, Mines and Resources Canada | Énergie, Mines et Ressources Canada

CANMET

Canada Centre for Mineral and Energy Technology | Centre canadien de la technologie des minéraux et de l'énergie

A PRELIMINARY TECHNICAL EVALUATION OF THE α-NUCLEAR ELECTRONIC PERSONAL DOSIMETER IN AN UNDERGROUND URANIUM MINE

J. BIGU & R. REGAN

ELLIOT LAKE LABORATORY

AUGUST 1980

This document is an unedited interim report prepared primarily for discussion and internal reporting purposes. It does not represent a final expression of the opinion of the Canada Centre for Mineral and Energy Technology (CANMET)

Ce document est un rapport provisoire non-révisé et rédigé principalement pour fin de discussion et de documentation interne. Il ne représente nullement l'expression définitive de l'opinion du Centre canadien de la technologie des minéraux et de l'énergie (CANMET)

48 pp

MINERALS RESEARCH PROGRAM
MINING RESEARCH LABORATORIES
DIVISION REPORT MRP/MRL 80-120(TR)

A PRELIMINARY TECHNICAL EVALUATION OF THE α-NUCLEAR ELECTRONIC PERSONAL DOSIMETER IN AN UNDERGROUND URANIUM MINE

by

J. Bigu* and R. Regan**

ABSTRACT

This report presents data on underground tests carried out in an Ontario uranium mine with a personal α-dosimeter of the electronic type designed and manufactured by Alpha-NUCLEAR, a firm based near Toronto. Experimental data have been compared with theoretical predictions. Fair agreement has been found between theoretical and experimental results. A number of suggestions are made to improve the performance of the dosimeter.

---

* Research Scientist and underground environment project leader, ** Technician, Elliot Lake Laboratory, Mining Research Laboratories, Canada Centre for Mineral and Energy Technology, Department of Energy, Mines and Resources, Elliot Lake, Ontario.

CONTENTS

ABSTRACT i
INTRODUCTION 1
THE ALPHA-NUCLEAR ELECTRONIC DOSIMETER 3
EXPERIMENTAL TESTS CARRIED OUT WITH THE α-NUCLEAR DOSIMETER 4
EXPERIMENTAL RESULTS 6
DISCUSSION 19
CONCLUSION AND FINAL REMARKS 23
ACKNOWLEDGEMENTS 24
REFERENCES 25

TABLES

1. Working levels and decay products concentrations 7
2. Working levels and ThB concentrations 10
3. Average experimental values for several radiation variables of interest 12
4. Dosimeter exposure and grab sampling data 13
5. 'Residual' α-activity on dosimeter filter due to the presence of thoron daughters 14
6. Average air flow, temperature and barometric pressure measurements 15
7. Experimental calibration factor (Kf) for two personal dosimeters 16

FIGURES

1. Dosimeter reading (α-count) versus $\overline{WL}$(Rn) x t for two dosimeters 27
2. Dosimeter reading versus time elapsed from the beginning of sampling 28
3. Dosimeter reading versus time elapsed from the beginning of sampling 29
4. Number of occurrences of the ratios [RaB]/[RaA] and [RaC]/[RaA] from the field data 30
5. Experimental values of [RaB]/[RaA] versus [RaC]/[RaA] on a graph showing the theoretical limiting boundaries for the above (theoretical) ratios for various mine models 31
6. Experimental normalized (relative to WL(Rn)) values of [RaA] and [RaB] 32

7. Theoretical number of α-counts due to radon daughters (N(Rn)), thoron daughters (N(Tn)) and total N_T as a function of a waiting time (T_w) of 240 min 33

8. Theoretical number of α-counts due to radon daughters (N(Rn)), thoron daughters (N(Tn)) and total N_T as a function of waiting time (T_w) for a sampling time (T_s) of 240 min 34

9. Theoretical number of α-counts due to radon daughters (N(Rn)), thoron daughters (N(Tn)) and total N_T as a function of waiting time (T_w) for a sampling time (T_s) of 240 min 35

10. Theoretical number of α-counts due to radon daughters (N(Rn)), thoron daughters (N(Rn)) and total N_T as a function of waiting time (T_w) for a sampling time (T_s) of 240 min 36

11. Theoretical number of α-counts due to radon daughters (N(Rn)), thoron daughters (N(Tn)) and total (N_T) as a function of sampling time (T_s) for a waiting time (T_w) of 180 min 37

12. Theoretical number of α-counts due to radon daughters (N(Rn)), thoron daughters (N(Tn)) and total N_T as a function of sampling time (T_s) for a waiting time (T_w) of 180 min 38

13. Theoretical number of α-counts due to radon daughters (N(Rn)), thoron daughters (N(Tn)) and total (N_T) as a function of sampling time (T_s) for a waiting time (T_w) of 180 min 39

14. Theoretical number of α-counts due to radon daughters (N(Rn)), thoron daughters (N(Tn)) and total (N_T) as a function of sampling time (T_s) for a waiting time (T_w) of 180 min 40

15. Theoretical total number of α-counts due to radon daughter activity as a function of sampling time for different daughter disequilibrium ratios 41

16. Theoretical total number of α-counts due to thoron daughter activity as a function of sampling time for different daughter disequilibrium ratios..... 42

17. Theoretical total number of α-counts due to thoron daughter activity as a function of sampling time for different daughter disequilibrium ratios 43

18. Flow rate of dosimeters α-1 and α-2 for a 3-day laboratory test 44

INTRODUCTION

Personal radiation dosimeters have been developed to estimate the exposure of occupational workers to different kinds of radiation.

Several personal α-particle dosimeters have been designed to determine the exposure of miners to α-radiation in underground uranium mines. Personal α-dosimeters are time-integrating devices that are usually calibrated in terms of α-radiation exposure, e.g., Working Level Month (WLM) or Working Level Hour (WLH). A personal α-dosimeter consists essentially of a highly efficient pump, a sampling head (housing an adequate filter) and an α-detector. Air is flowed through the filter where the decay products of radon (and thoron) are deposited. α-particles emitted by the α-emitters RaA and RaC' (and also ThC and ThC') are detected by an appropriate detector, e.g., a thermoluminescent detector (TLD), a track etch detector (e.g., cellulose nitrate) or a silicone diffused or surface barrier detector. According to the kind of detector used,personal α-dosimeters have come to be known as TLD dosimeters (TLDD), track etch dosimeters (TED) or solid-state (electronic) dosimeters (SSED). Some of these dosimeters are still under continuous research and development or technical evaluation in uranium mines.

The need for a reliable α-dosimeter has been recognized for some time. However, there is no single personal dosimeter that combines the broad spectrum of practical requirements including: being inexpensive to build, rugged, simple to maintain and retrieve information from, has long time reliability, and is, in addition, responsive to the ever growing need for discriminating the thoron progeny present in relatively high amounts in some Canadian uranium mines. Some of the characteristics of the dosimeters referred to above are given below for the benefit of the reader:

A. TLD Dosimeters (1 to 5)

a) TLD chips are cheap and re-useable, but respond to different types of radiation (e.g., α, β, γ, UV, light) with different sensitivity. Thus more than one chip and shielding is necessary to determine α-dose. Reading of TLD chip is usually done after exposure to radiation for several days or weeks at a time;

b) TLD chips require careful handling as they are very sensitive to light, heat and some environmental factors. Some materials exhibit a phenomenon called 'fading';

c) Once the information stored in the TLD chip is 'read' the information is lost;

d) Discrimination of thoron decay products is difficult.

B. Track Etch Dosimeter (CEA* Dosimeter)(6)

a) Insensitive to γ-radiation, hence no unwanted background;

b) Detector (i.e., cellulose nitrate) is cheap;

c) New dosimeter design enables discrimination of thoron progeny;

d) Detector requires chemical etching, a process which is time consuming and cumbersome. For large numbers of samples a highly automated 'reading' system, such as the Quantimet Image Analyzing Computer is needed which makes initial investment rather high. Reading of detector is usually done after exposure to radiation for several days or weeks at a time.

C. Solid-State/Electronic Detectors (7,8)

a) Detector (Silicon diffused or surface barrier detector) and associated electronic circuitry is relatively expensive;

b) Information (WLH or α-counts) is directly read daily by means of an electronic reader in a matter of a few seconds;

---

* Commissariat à l'Energie Atomique.

c) Information can be retrieved at any chosen moment without loss of the information except, as in the case of Alpha NUCLEAR, when unplugged from the reader;

d) Discrimination of thoron decay products is possible by taking more than one reading on the same sample after the radon decay products have decayed away.

The choice of one dosimeter type over another must be based on a number of factors including long-term reliability, ruggedness, initial investment and routine maintenance, ease of operation and data processing and retrieval. In spite of the obvious benefit of personal α-dosimeters in the estimation of exposure of uranium miners their use is not widespread there being only a few mines where α-dosimeters are employed on a routine basis.

This report presents data on underground tests carried out in an Ontario uranium mine with a personal α-dosimeter of the electronic type designed and manufactured by Alpha NUCLEAR, a firm based near Toronto, Ontario.

THE ALPHA-NUCLEAR ELECTRONIC DOSIMETER

The dosimeter is a compact, rugged and lightweight unit consisting of a sampling head, housing an α-detector, and a filter, associated electronic circuitry and a sampling pump. The detector is a Silicon Diffused Junction type of 400 mm^2 sensitive area, protected from plate-out contamination by a thin metallized mylar sheet. The constant flow (approximately 100 cc/min) pump continuously draws air through a fiber glass or 0.8 μm Millipore filter facing the α-detector. The airborne radon and thoron decay products are deposited in the filter and their disintegration is counted by the detector, amplified and stored within the memory. The dosimeter memory has the capability of storing 1×10^6 α-counts, which is approximately equivalent to 37.5 WLH of radon

daughters. The dosimeter detects in real time.

The dosimeter operates in conjunction with a standard miner's cap lamp battery to which it fits snuggly. The unit is worn around the belt and has no external controls, which prevents the unit from being accidentally misused. The filter is changed everyday before the shift and the data are 'read' after the shift by means of a microprocessor-controlled electronic reading network (reader), located on 'surface'.

The reader provides the controlling functions for the dosimeter. When the reader is plugged into the dosimeter the pump automatically switches off. When the reader is unplugged, the pump switches on, the data on the dosimeter memory are erased, i.e., reset to zero, and a new counting period is started. After the end of sampling the reader is again plugged into the dosimeter and the accumulated data, i.e., α-counts, during the sampling period can be read. In a modified, more advanced version of the dosimeter reader system, data transfer can be carried out automatically 3 1/2 hours after the end of sampling, for radon daughters, and at a later time, programmable, for thoron daughters. The data is printed automatically by a thermal printer.

The reader also displays the serial number of the dosimeter, which is electronically implanted, for the purpose of identification.

EXPERIMENTAL TESTS CARRIED OUT WITH THE α-NUCLEAR DOSIMETER

A number of tests were carried out. The tests were divided into two parts: laboratory tests and underground tests in a uranium mine. The laboratory tests consisted of:

a) Pump flow-rate measurements and studies of the constancy and reproducibility of the flow-rate for a period of several days;

b) Determination of the detector's efficiency. Measurements were carried

out with a standard Am-241 source;

c) Response of the detector system to cosmic radiation and environmental radioactive airborne contaminants. This study was conducted with no filter in the dosimeter's head.

Underground tests were aimed at investigating the performance of the dosimeter:

a) For various mining units operations - mainly slushing, drilling and roof-bolting;

b) At different mine locations including inactive mining areas (e.g., garage, where high diesel particulate concentrations were found) and active working stopes (see item (a)).

Concurrent with the dosimeter underground tests, the following side by side measurements were carried out:

i) radon gas concentration;

ii) concentrations in mine air of the short-lived radon decay products RaA, RaB, RaC and RaC';

iii) radon daughters Working Level, i.e., WL(Rn);

iv) concentration in mine air of thoron daughters, e.g., ThB;

v) thoron daughters Working Levels, i.e., WL(Tn);

vi) γ-activity arising from K-40 and the Th-232 and U-238 decay chains;

vii) aerosol size distribution;

viii) unattached decay products fraction;

ix) meteorological variables including temperature and barometric pressure;

x) air flow, i.e., ventilation characteristics.

Because some underground uranium mines have thoron gas, and therefore, thoron decay products in amounts substantially higher than originally predicted

or anticipated, the response of personal α-dosimeters in radon/thoron daughter mixtures is of utmost importance if the health hazards derived from exposure to these products is to be properly evaluated. Items (i) through (v) in conjunction with item (x) were partly aimed at studying the response of the dosimeter to varying mixtures of radon and thoron daughters.

The WL of radon daughters was determined by three different methods (using the same sample): the Kusnetz method (9,10), the Thomas method (11) and the Markov method (12). Radon daughter concentrations were measured by the Thomas method. Radon daughter measurements including the WL were corrected to account for the presence of thoron daughters. Thoron daughter WLs were calculated according to the Kusnetz technique, i.e., single gross α-count. Measurements were carried out (on the same samples used to determine radon daughters concentrations and WLs) 7 to 10 hours after sampling. ThB concentrations were derived from single gross α-counts according to routine procedures.

The dosimeter was read (by the dosimeter read-out unit) 3 hours after the end of sampling and at regular intervals thereafter in order to 'isolate' the thoron daughter concentration to the total α-dose. After the dosimeter readings were completed the filter was removed and its α-activity counted. Experimental data were compared with theoretical predictions as shown below.

Radon gas measurements were carried out by conventional techniques 3 to 4 hours after taking samples in scintillation cells.

Underground tests were conducted at an Elliot Lake (Ontario) underground uranium mine for a period of approximately 3 weeks.

EXPERIMENTAL RESULTS

Table 1 shows the radon daughter and thoron daughter WLs and the activity concentrations (indicated by square brackets) of RaA, RaB, RaC and

Table 1 - Working levels and decay products concentrations

Date	Location	$WL(Rn)_{Th}$	$WL(Rn)_{K}$	$WL(Rn)_{M}$	[RaA] (pCi/L)	[RaB] (pCi/L)	[RaC] (pCi/L)	$\frac{[RaB]}{[RaA]}$	$\frac{[RaC]}{[RaA]}$	WL(Tn)	[ThB] (pCi/L)	Time of Measurement	Mining Operation
Nov. 14	Garage	0.578	0.586	-	100.86	61.85	42.95	0.61	0.43	0.338	2.72	9.50	
	"	0.561	0.548	-	98.67	62.32	38.38	0.63	0.39	0.327	2.64	10.38	
	"	0.569	0.575	-	95.76	63.12	40.33	0.66	0.42	0.329	2.67	11.33	
	"	0.547	0.552	-	82.92	59.03	43.36	0.71	0.52	0.343	2.79	12.13	
	"	0.586	0.603	-	90.55	63.13	46.11	0.70	0.51	0.358	2.92	12.58	
Nov. 15	Garage	0.583	0.598	-	88.15	62.97	46.15	0.71	0.52	0.368	2.95	10.08	
	"	0.594	0.594	0.599	93.98	66.10	43.37	0.70	0.46	0.370	2.99	10.53	
	"	0.614	0.611	0.616	98.85	67.10	46.00	0.68	0.46	0.383	3.10	11.38	
	"	0.588	0.598	0.604	91.25	64.45	44.86	0.71	0.49	0.349	2.84	12.24	
	"	0.593	0.615	0.610	86.55	65.17	46.44	0.75	0.54	0.368	2.99	13.09	
Nov. 16	Garage	0.550	0.564	0.551	85.14	60.35	41.83	0.71	0.49	0.330	2.69	9.21	
	"	0.570	0.563	0.579	98.22	62.01	41.28	0.63	0.42	0.351	2.83	10.07	
	"	0.562	0.565	0.582	87.65	61.47	42.93	0.70	0.49	0.351	2.84	10.52	
	"	0.505	0.536	0.530	70.83	53.88	42.39	0.76	0.60	0.343	2.80	11.38	
	"	0.480	0.477	0.493	79.37	52.17	35.91	0.66	0.45	0.359	2.91	12.23	
Nov. 19	Garage	0.594	0.608	0.608	92.42	64.03	46.31	0.69	0.50	0.367	2.96	10.13	
	"	0.568	0.569	0.575	94.73	62.73	40.75	0.66	0.43	0.373	3.02	10.58	
	"	0.531	0.537	0.532	86.90	58.88	38.26	0.68	0.44	0.362	2.94	11.43	
	"	0.540	0.545	0.537	88.39	59.63	39.13	0.67	0.44	0.349	2.84	12.28	
	"	0.509	0.517	0.528	80.44	54.99	39.52	0.68	0.49	0.364	2.97	13.14	
Nov. 20	Stope	0.422	0.428	0.426	76.64	45.08	30.76	0.59	0.40	0.205	1.66	9.43	
	"	0.556	0.571	0.579	97.84	57.95	43.24	0.59	0.44	0.285	2.30	10.29	
	"	0.549	0.562	0.571	94.24	58.30	41.86	0.62	0.44	0.299	2.42	11.14	Drilling
	"	0.610	0.585	0.607	117.19	67.46	39.42	0.57	0.34	0.289	2.34	11.59	
	"	0.476	0.468	0.469	89.64	53.38	30.21	0.59	0.34	0.241	1.96	12.50	
Nov. 21	Stope	0.455	0.437	0.436	95.74	50.73	26.54	0.53	0.28	0.235	1.90	9.49	
	"	0.456	0.466	0.469	81.71	48.21	34.08	0.59	0.42	0.271	2.19	10.34	
	"	0.571	0.585	0.597	95.30	59.62	45.62	0.63	0.48	0.282	2.29	11.18	Drilling
	"	0.520	0.545	0.529	102.00	55.41	35.82	0.54	0.35	0.274	2.23	12.04	
	"	0.488	0.506	0.483	89.26	52.74	34.32	0.59	0.38	0.256	2.08	12.48	

Cont. overleaf

Table 1 - Working levels and decay products concentrations (Con't.)

Date	Location	$WL(Rn)_{Th}$	$WL(Rn)_{K}$	$WL(Rn)_{M}$	[RaA] (pCi/L)	[RaB] (pCi/L)	[RaC] (pCi/L)	$\frac{[RaB]}{[RaA]}$	$\frac{[RaC]}{[RaA]}$	WL(Tn)	[ThB] (pCi/L)	Time of Measurement	Mining Operation
Nov. 22	Stope	0.571	0.565	0.588	91.11	62.16	43.26	0.68	0.47	0.275	2.23	9.31	
	"	0.749	0.733	0.766	140.61	79.92	53.13	0.57	0.38	0.272	2.36	10.15	
	"	0.626	0.636	0.632	114.39	67.02	45.10	0.59	0.39	0.312	2.53	11.01	Slushing
	"	0.650	0.655	0.674	111.43	68.54	50.23	0.61	0.45	0.275	2.24	11.45	
	"	0.664	0.661	0.676	127.40	71.09	46.21	0.56	0.36	0.301	2.45	12.31	
Nov. 23	Stope	0.462	0.476	0.481	78.29	48.79	35.93	0.62	0.46	0.269	2.17	9.19	Slushing,
	"	0.474	0.478	0.488	91.47	49.26	34.76	0.54	0.38	0.253	2.04	10.04	drilling,
	"	0.487	0.480	0.500	93.09	52.15	33.91	0.56	0.36	0.295	2.39	10.49	roof-bolt-
	"	0.518	0.515	0.525	99.98	54.44	37.30	0.54	0.37	0.279	2.26	11.35	ing and
	"	0.461	0.455	0.427	90.82	49.06	31.67	0.54	0.35	0.257	2.09	12.24	scaling
Dec. 3	Stope	0.540	0.537	0.538	112.74	57.76	34.97	0.51	0.31	0.327	2.63	9.26	
	"	0.588	0.602	0.593	117.04	62.04	40.86	0.53	0.35	0.365	2.94	10.12	
	"	0.583	0.587	0.566	119.40	65.33	34.48	0.55	0.29	0.362	2.93	10.56	Drilling
	"	0.528	0.531	0.528	108.47	58.41	32.24	0.54	0.30	0.345	2.81	11.41	
	"	0.339	0.332	0.333	85.41	36.01	18.39	0.42	0.21	0.250	2.04	12.27	
Dec. 4	Slusher Bench	0.054	0.052	0.060	19.56	4.62	2.94	0.24	0.15	0.156	1.26	9.32	
	"	0.057	0.054	0.058	19.21	5.36	2.68	0.28	0.14	0.177	1.42	10.16	
	"	0.056	0.054	0.055	18.99	5.18	2.71	0.27	0.14	0.180	1.45	11.02	Slushing
	"	0.060	0.054	0.057	20.81	6.41	1.66	0.31	0.08	0.165	1.37	11.48	
	"	0.050	0.054	0.049	16.70	4.53	2.75	0.27	0.16	0.162	1.32	12.34	
Dec. 7	Stope	0.117	0.105	0.118	35.72	11.32	6.06	0.32	0.17	0.192	1.53	9.14	Drilling
	"	0.120	0.120	0.117	34.93	11.70	6.58	0.33	0.19	0.200	1.61	10.24	and
	"	0.129	0.134	0.128	37.15	13.05	6.46	0.35	0.17	0.224	1.81	11.15	Roof-
	"	0.129	0.124	0.120	38.84	12.90	6.19	0.33	0.16	0.203	1.65	12.05	bolting
	"	0.117	0.110	0.112	36.95	11.94	5.00	0.32	0.13	0.163	1.33	12.55	

ThB as determined at different mine locations, dates and times. The subindices Th, K and M stand, respectively, for Thomas, Kusnetz and Markov and indicate the method used to determine the WL. The Table also shows the mining operation.

Table 2 shows the radon daughter and thoron daughter WLs and the ThB activity concentrations as determined at different mine locations, dates and times. The data shown in Tables 1 and 2 were obtained by two different operators and experimental set-ups. The Table also shows the mining operation.

Table 3 shows the average experimental values of [RaA], [RaB], [RaC], [ThB], WL(Rn)/WL(Tn), [RaB]/[RaA] and [RaC]/[RaA] obtained for different mine locations which have been used for the theoretical computations shown below (see Figs 7 to 17). The data collected for the working stope have been divided into two groups according to the ventilation observed.

Table 4 shows relevant data pertaining to the dosimeter; it includes dosimeter sampling time, dosimeter reading, underground WLs for radon and thoron daughters and radon daughter radiation exposure in WLH.

Table 5 shows the 'residual' α-activity on the dosimeter filter due to the presence of thoron daughters. The Table indicates the time elapsed from the beginning of sampling to the time of measurement. To obtain the number of α-counts (e.g., c.p.m.) that would be recorded by the dosimeter the figures given in the Table should be divided by the counting efficiency of the dosimeter's detector.

Table 6 shows the average values of the air flow, temperature and barometric pressure measured during the underground testing.

Table 7 shows the experimental calibration factor (K_f), defined below, for two different environmental conditions: 'old' mine air with high ratio WL(Rn)/WL(Tn) and 'young' mine air with low ratio WL(Rn)/(WL(Tn).

Figure 1 shows the dosimeter reading versus the quantity $\overline{WL}(Rn)$ x time

Table 2 - Working levels and ThB concentrations

Date	Location	$WL(Rn)_K$	$WL(Rn)_M$	WL(Tn)	[ThB] (pCi/L)	Time of Measurement	Mining Operation
Nov. 14	Garage	0.586	0.594	0.341	2.78	9.50	
		0.623	0.629	0.339	2.76	10.14	
		0.623	0.636	0.378	3.06	11.04	
		0.620	0.637	0.385	3.12	11.54	
		0.562	0.704	0.376	3.06	12.44	
		0.576	0.557	0.343	2.80	13.30	
Nov. 15	Garage	0.664	0.657	0.359	2.92	10.09	
		0.644	0.675	0.400	3.26	10.30	
		0.644	0.628	0.397	3.20	11.20	
		0.664	0.659	0.316	2.56	12.10	
		0.616	0.609	0.382	3.10	13.00	
		0.716	0.606	0.415	3.38	13.50	
Nov. 16	Garage	0.608	0.626	0.357	2.90	9.22	
		0.636	0.639	0.338	2.73	9.45	
		0.590	0.610	0.386	3.10	10.35	
		0.554	0.562	0.307	3.02	11.25	
		0.564	0.554	0.347	2.82	12.15	
		0.539	0.559	0.360	2.93	13.05	
Nov. 19	Garage	0.641	0.639	0.387	3.11	10.12	
		0.617	0.636	0.372	2.99	10.35	
		0.587	0.589	0.348	2.82	11.25	
		0.578	0.601	0.394	3.20	12.15	
		0.618	0.611	0.398	3.24	13.05	
		0.612	0.619	0.397	3.30	13.55	
Nov. 20	Stope	0.526	0.515	0.240	1.94	9.40	
		0.470	0.487	0.191	1.54	10.00	
		0.590	0.587	0.266	2.16	10.50	Drilling
		0.577	0.597	0.303	2.44	11.40	
		0.550	0.557	0.250	2.03	12.30	
		0.618	0.624	0.297	2.42	13.20	
Nov. 21	Stope	0.562	0.546	0.265	2.15	9.30	
		0.576	0.573	0.286	2.28	9.55	
		0.589	0.597	0.321	2.58	10.50	Drilling
		0.665	0.681	0.341	2.76	11.40	
		0.552	0.558	0.298	2.42	12.30	
		0.547	0.548	0.331	2.69	13.20	
Nov. 22	Stope	0.742	0.762	0.343	2.74	9.30	
		0.679	0.685	0.339	2.72	9.50	
		0.847	0.871	0.362	2.89	10.40	Slushing

Cont. overleaf

Table 2 - Working levels and ThB concentrations (cont.)

Date	Location	$WL(Rn)_K$	$WL(Rn)_M$	WL(Tn)	[ThB] (pCi/L)	Time of Measurement	Mining Operation
Nov. 22	Stope	0.781	0.801	0.344	2.79	11.30	Slushing
		0.762	0.770	0.332	2.70	12.20	
		0.686	0.687	0.301	2.45	13.10	
Nov. 23	Stope	0.574	0.578	0.313	2.52	9.15	Slushing, Drilling, Roof-bolting and Scaling
		0.540	0.552	0.259	2.09	9.35	
		0.546	0.561	0.315	2.52	10.25	
		0.660	0.655	0.318	2.57	11.15	
		0.597	0.626	0.331	2.68	12.05	
		0.500	0.515	0.305	2.77	12.55	
Dec. 3	Stope	0.625	0.619	0.374	2.98	9.25	Drilling
		0.674	0.646	0.350	2.78	9.45	
		0.708	0.674	0.387	3.12	10.35	
		0.584	0.586	0.355	2.88	11.25	
		0.341	0.326	0.282	2.29	12.05	
		0.307	0.337	0.260	2.12	13.05	
Dec. 4	Slusher Bench	0.062	0.057	0.179	1.50	9.30	Slushing
		0.063	0.053	0.160	1.34	9.50	
		0.055	0.050	0.185	1.51	10.40	
		0.055	0.053	0.176	1.42	11.30	
		0.064	0.061	0.170	1.38	12.20	
		0.058	0.058	0.163	1.33	13.10	

Table 3 - Average experimental values for several radiation variables of interest

Location	[RaA] (pCi/L)	[RaB] (pCi/L)	[RaC] (pCi/L)	[ThB] (pCi/L)	$\frac{[RaA]}{[RaA]} : \frac{[RaB]}{[RaA]} : \frac{[RaC]}{[RaA]}$	WL(Rn)/WL(Tn)	Remarks
Garage	89.58	61.27	42.32	2.87	1 : 0.68 : 0.47	1.60	poor ventilation
Stope	100.84	57.23	37.37	2.30	1 : 0.57 : 0.37	1.90	poor ventilation
Slusher's Bench	19.05	5.22	2.55	1.36	1 : 0.27 : 0.13	0.31	good ventilation
Stope	36.72	12.18	6.06	1.59	1 : 0.33 : 0.16	0.60	good ventilation

Table 4 - Dosimeter exposure and grab sampling data

Date	Location	Dosimeter number	Sampling time, T_s [hr]	Dosimeter reading [α-counts] ++	Daily average WL(Rn)	$\overline{WL(Rn)} \times T_s$ [WLH]	WL(Tn)	W_t = WL(Rn)+ WL(Tn)	$\frac{WL(Rn)}{WL(Tn)}$	Mining Operation	Remarks
Nov. 14	Garage	α-2	4.53	70100	0.573	2.60	0.339	0.91	1.69	Diesel trucks	
Nov. 16	"	α-2	4.27	65900	0.541	2.31	0.347	0.89	1.56	"	
Nov. 19	"	α-2	4.50	71534	0.556	2.50	0.363	0.92	1.53	"	
Nov. 20	Stope	α-2	4.50	Did not work	0.523	2.35	0.264	0.79	1.98	Drilling	Low air flow
Nov. 21	"	α-1	4.70	65444	0.508	2.39	0.264	0.77	1.92	Drilling	
Nov. 21	"	α-2	4.70	57340	0.508	2.39	0.264	0.77			
Nov. 22	"	α-1	4.57	77644	0.65	2.97	0.287	0.94	2.26	Slushing*	
Nov. 22	"	α-2	4.57	68155	0.65	2.97	0.287	0.94		"	
Nov. 23	"	α-1	4.53	61803	0.481	2.18	0.271	0.75	1.77	Slushing, drilling, roof bolting & scaling	
Nov. 23	"	α-2	4.53	49612	0.481	2.18	0.271	0.75			
Dec. 3	"	α-1	4.53	59687	0.518	2.35	0.33	0.85	1.57	Drilling	
Dec. 3	"	α-2	4.53	10948**	0.518	2.35	0.33	0.85		"	
Dec. 4	Slusher Bench	α-1	4.5	9758	0.053	0.238	0.168	0.22	0.31	Slushing+	High air flow
Dec. 4	"	α-2	4.5	7512	0.053	0.238	0.168	0.22		"	
Dec. 7	Stope	α-1	4.9	29356	0.118	0.578	0.196	0.31	0.60	Drilling &	
Dec. 7	"	α-2	4.9	16558	0.118	0.578	0.196	0.31		roof bolting	

Data on α-2 for Nov. 15 was accidentally erased.

* Sampling upstream

** Pump Malfunction

\+ Sampling downstream

++ Not corrected for flow-rate

Table 5 - 'Residual' α-activity on dosimeter filter due to the presence of thoron daughters

Date	Location	Dosimeter Number	Waiting Time [hr]	dpm
Nov. 14	Garage	α-1	11.00	107.5
Nov. 14	"	α-2	11.1	93.5
Nov. 15	"			
Nov. 15	"			
Nov. 16	"	α-1		
Nov. 16	"	α-2	10.92	108.1
Nov. 19	"	α-1	10.75	116.6
Nov. 19	"	α-2	10.83	96.0
Nov. 20	Stope	α-1		
Nov. 20	"	α-2	11.42	59.5
Nov. 21	"	α-1	11.18	83.6
Nov. 21	"	α-2	11.18	69.5
Nov. 22	"	α-1	11.17	90.9
Nov. 22	"	α-2	11.33	74.7
Nov. 23	"	α-1	11.27	88.6
Nov. 23	"	α-2	11.40	56.5
Dec. 3	"	α-1	11.13	102.4
Dec. 3	"	α-2	11.30	19.0
Dec. 4	Slusher Bench	α-1		Non Measurable
Dec. 4	"	α-2		"
Dec. 7	Stope	α-1	7.50	19.5
Dec. 7	"	α-2	8.00	11.8

Table 6 - Average air flow, temperature and barometric pressure measurements

Date	Location	P_u(mb)	T(°C)	Q(m^3/sec)	P_s(mb)
Nov. 14	Garage	1033.59	12.7	≷ 3.5	979.70
Nov. 15	"	1018.60	12.3	"	972.38
Nov. 16	"	1028.07	12.4	"	Not measured
Nov. 19	"	1025.96	12.3	"	973.90
Nov. 20	Stope	1025.37	11.7	≃ 3.5	984.34
Nov. 21	"	1033.58	11.6	"	982.82
Nov. 22	"	1023.74	12.0	"	974.90
Nov. 23	"	1013.97	11.7	"	968.90
Dec. 3	"	1021.79	11.6	"	970.56
Dec. 4	Slusher's Bench	1023.27	11.4	13.1	971.87
Dec. 7	Stope	999.74	10.63	7.7	951.63

P_u, P_s, T and Q stand, respectively, for underground barometric pressure, surface barometric pressure, temperature and air flow.

Table 7 - Experimental calibration factor (K_f) for two personal dosimeters

Dosimeter No.	Dosimeter Reading+ (Total α-count)	$\overline{WL(Rn)} \times T_s$ (WLH)	K_f	$\overline{K_f}$*	Remarks
α-1	65444	2.39	280	275	'Old Air' (40-60 min)
	77644	2.97	268		
	61803	2.18	290		
	59687	2.35	260		
	9758	0.238	420	470	'Young Air' (20-25 min)
	29356	0.578	520		
α-2	70100	2.60	270	278	'Old Air' (40-60 min)
	65900	2.31	285		
	71534	2.50	286		
	65430	2.39	274		
	77321	2.97	260		
	61980	2.18	284	443	'Young Air' (20-25 min)
	10803	0.238	454		
	25010	0.578	433		

+ Normalized to 100 cc/min (α-count includes thoron daughters contribution).

* Average K_f.

where the time is given in hours and $\overline{WL}$(Rn) stands for the average radon daughter WL measured during the dosimeter sampling time (see Tables 1, 1 and 4).

Figures 2 and 3 show the dosimeters readings (i.e., total α-count) for α-1 and α-2 taken on December 4th and 7th versus the time (t) elapsed from the beginning of sampling. Theoretical graphs have also been plotted for comparison purposes. The dosimeter's reading as a function of the time elapsed from the end of sampling is simply obtained by reading the α-count at a time $t-T_s$ where T_s is the sampling time, usually about 4 hours in our case. Notice that for times equal to or greater than $t - (T_s + T_w)$, where T_w (i.e., waiting time) is the time elapsed between the end of sampling and the dosimeter reading, the α-count should remain constant, for $T_w \simeq 3.5$ hours, if only radon daughters were present in the filter. The fact that the α-count continues to increase for times greater than $t - (T_s + T_w)$ clearly indicates the presence of thoron daughters in the mine atmosphere.

Figure 4 shows the number of occurrences of the ratios [RaB]/[RaA] and [RaC]/[RaA] from the field data.

Figure 5 gives the experimental values of [RaC]/[RaA] versus [RaB]/[RaA] on a graph showing the theoretical limiting boundaries for the same (theoretical) ratios for various mine models: the mine tunnel (curve Y), the isolated system (curve X) and a mine model consisting of the mixing of 'young' and 'old' air (curve Z) (13,14). Note: the isolated system is defined as one in which a certain quantity of radon gas is added initially to pure air and then decays, there being no replenishment or removal of activity from the system. In the mine-tunnel model a source of radon is released at one point in the mine and then carried along with the ventilation air through the rest of the mine. The radon gas is constantly replenished by diffusion from the walls of the mine.

Figure 6 shows the experimental normalized (relative to WL(Rn)) values of [RaA] versus [RaB]. Solid and broken lines represent theoretical

values. For a description of this type of graph see (15,16,17). The method to calculate the theoretical normalized radon daughter concentrations has been discussed by Evans (18).

Figures 7, 8, 9 and 10 show the theoretical number of α-counts (sampling plus waiting) that would be recorded by a personal dosimeter with a detector efficiency ε and pump flow rate Q [L/min] due to:

a) radon daughters, N(Rn)

b) thoron daughters, N(Tn)

c) radon daughters plus thoron daughter, N_T

as a function of waiting time, for a sampling time of 240 minutes, for different states of radon daughter disequilibrium: 1:0.63:0.47 (garage, low air flow); 1:0.57:0.37 (stope, low air flow) and approximately 1:0.3:0.15 (slushers bench and stope, high air flow). For simplicity the results have been 'normalized' to ε = 1.0 and Q = 0.1 L/min. To obtain the actual values, N(Rn), N(Tn) and N_T should be multiplied by the corresponding values of ε(≈0.19) and Q. The details of the above calculations are given in a forthcoming report (19).

Figures 11, 12, 13 and 14 are similar to Fig. 7 to 10 except that ((Rn), N(Tn) and N_T are given as a function of sampling time for a waiting time of 180 minutes, (Note: the activity remaining on the filter due to radon daughters is negligibly small 180 minutes after the end of sampling.)

Figures 15, 16 and 17 show the total radon (thoron) daughter activity on the filter (ε=1, Q=0.1 L/min) as a function of sampling time for a waiting time of 180 minutes for several states of radon (thoron) daughter disequilibrium.

Figure 18 shows the flow rate of the dosimeter pumps during a 3-day laboratory test. Note: pump flow rate measurements were made daily during the underground tests. The performance of pump No. 2 (dosimeter α-2) was found unsatisfactory: it decreased to less than 75% of its original preset

value of 0.1 L/min after a few days of underground testing. Because of the pump's poor performance no attempt was made to reset the pump flow rate daily, but rather to 'follow' its flow.

DISCUSSION

The underground tests were conducted in three mine locations: a garage, a working stope and an area at the bottom of the stope where a slusher was located. An analysis of the radiation data in these locations indicates two well defined sets of conditions:

1. A condition characterized by 'old' air (40-60 min), as a result of low air flow in the area, and hence high ratios of [RaB]/[RaA] and [RaC]/[RaA] ranging, respectively, from 0.57 to 0.68 and 0.37 to 0.47 of relatively high activity (90-100 pCi/L of RaA) and moderate WL(Tn) contribution (WL(Rn)/WL(Tn) = 1.60 to 1.90); and
2. A condition characterized by 'young' air (20-25 min) with low ratios of [RaB]/[RaA] and [RaC]/[RaA] ranging, respectively, from 0.27 to 0.33 and 0.13 to 0.16 of low activity (20-36 pCi/L of RaA) and high WL(Tn) contribution (WL(Rn)/WL(Tn) = 0.3 to 0.6).

The above average conditions are summarized in Table 3, from data given in Tables 1 and 2, and Fig. 4, 5 and 6.

Calibration of the dosimeters is carried out according to the following Equation:

$$\overline{WL(Rn)}\ T_s = N_{\alpha,T}/Q\ \epsilon\eta \qquad \text{Eq 1}$$

where: $\overline{WL(Rn)}$ is the average radon daughter WL to which the dosimeters are exposed

T_s is the dosimeter sampling time

$N_{\alpha,T}$ is the total number of α-counts recorded by the dosimeter

Q is the flow rate of the dosimeter pump

ε is the efficiency of the dosimeter detector head for a given filter type/detector geometry

η is a factor that takes into account filter collecting efficiency, plate-out effects, and so on.

Calling $\overline{WL(Rn)}\ T_s$ = WLH and $\varepsilon\eta = K_f$, an overall calibration factor, the dosimeters can be calibrated by means of the expression:

$$K_f = N_{\alpha,T}/Q \times WLH \qquad \text{Eq 2}$$

The values of WLH, calculated from WL data shown in Tables 1 and 2, and $N_{\alpha,T}$ are given in Table 4. Fig. 1 shows that the relationship of the 'normalized' (for Q = 100cc/L) $N_{\alpha,T}$ and WLH can be described by a straight line of slope 23647 α-counts WLH^{-1} intersecting the $N_{\alpha,T}$ axis at 8898 counts. The data point marked (?) has been discarded due to pump malfunction.

The experimental values obtained for K_f, calculated with Equation 2, are given in Table 7. Two average values of K_f, i.e., $\overline{K}_f$, are found depending upon experimental conditions: a lower value of 276 $\pm$ 11 for 'old' air (40-60 minutes) and relatively low WL(Tn) contribution, and a higher value of 457 $\pm$ 44 for relatively 'young' air (20-25 minutes) with high WL(Tn) contribution (see Tables 3 and 7).

The increase in the value of K_f with decreasing ratio WL(Rn)/WL(Tn), i.e., increasing thoron daughter contribution, is theoretically predictable. Theoretical values for K_f can be calculated with the aid of the theoretical data given in Fig. 7 to 17 for the radon (and thoron) daughter ratios and activities of interest here. Alternatively, the expected number of α-counts recorded by a dosimeter with a flow rate Q and α-particle efficiency ε can be obtained with the same data, and compared with experimental values. However, an accurate comparison of experimental and theoretical data would require

graphs for all the radon (and thoron) daughter ratios and activities, and dosimeter sampling times encountered in the course of the underground tests (see Tables 1 and 4). (Due to space and time limitations only part of these data are produced here. A comprehensive theoretical analysis of the data will be given in a forthcoming report.) In order to compare the experimental data shown in Tables 3, 4 and 7, and Fig. 1 with theoretical data the graphs(s) corresponding to the decay products state of disequilibrium, and [RaA] and [ThB] of interest should be multiplied by the product $Q\varepsilon$ where Q varied between 0.07 L/min and 0.1 L/min and ε, for the dosimeters tested, was approximately 0.19. Some of the complicating factors which makes comparison of theoretical and experimental values somewhat time consuming, cumbersome and at times difficult are listed below:

a) The dosimeter sampling time at the locations of interest varied from day to day from 240 min to 300 min (see Table 4). Moreover, the dosimeters pumps could not be switched off after the sampling period without erasing the data stored in the memory. Thus a fraction of the dosimeter reading originated during the time elapsed from the end of true sampling to the time of arrival in the laboratory where the reader was plugged in to the dosimeters thereby stopping their pumps. During this travel time (i.e., ca. 20 min from the sampling site to the 'cage', 15 min to get to surface, 30 min to arrive at the laboratory) the dosimeter was exposed to different, unknown, WL(Rn) and WL(Tn). However, and for all practical purposes, the contribution to the total dose arising from the surface environment can be considered small compared to the contribution arising from the sampling site to the cage. An estimated uncertainty of the order of 20% in the dosimeter read ng is attributed to the above factors;

b) The radon daughter ratios, i.e., [RaB]/[RaA] and [RaC]/[RaA], and daughter

activities - and hence WL(Rn) - varied from day to day and during the sampling period depending upon environmental conditions and mining operations (see Tables 1, 2 and 4);

c) The thoron daughter ratio [ThC]/[ThB], daughters activities - and hence WL(Tn) - varied from day to day and during the sampling time depending upon environmental conditions and mining operations (see Tables 1, 2 and 4). As a consequence of items (b) and (c) the ratio WL(Rn)/WL(Tn) also varied. (see Tables 3 and 4). (Note: as only [ThB] measurements were conducted, i.e., [ThC] was not determined, the important ratio [ThC]/[ThB] is not known. Theoretical calculations for several mine models show, however, that [ThB] > [ThC]. The isolated model on the other hand shows that for an age of air equal to or greater than about 200 min the trend reverses, i.e., [ThC] > [ThB]. For the sake of simplicity we have assumed here equilibrium conditions for the thoron progeny (Fig. 7 to 10). A detailed analysis of this matter will be given in a forthcoming report (20).

d) The daily variation in the dosimeter flow rate amounted to as much as 20% of the mean value;

e) Routine radon (and thoron) daughter sampling could not always be conducted under the same conditions, (e.g., location) as the dosimeter sampling, particularly when the latter was worn by the miner;

f) The efficiency of the dosimeter's detector to α-particles is energy dependent and is therefore expected to be different for α-particles emitted by RaA and ThC (about 6 MeV) and RaC' (7.69 MeV). For the sake of simplicity, however, the efficiency has been taken as that corresponding to Am-241 (5.5 MeV), a source of which was used for calibration purposes. The efficiency of the detectors to 5.5 MeV α-particles was measured to be approximately 0.19.

g) Filter self-absorption and plate-out effects have been ignored, i.e., $\eta=1$ (see Eq. 1). Moreover, a potential source of experimental error regarding the filter should be pointed out: namely, tightening the top end of the filter head (which holds the filter tight to a narrow metal rim inset) beyond a certain point can break the filter around the edge of the rim, thereby allowing air flow around the rim rather than through the filter. This problem has been encountered when using fibreglass filters.

In spite of items (a) to (g), fair agreement was found in most cases between experimental and theoretical values (see for example Fig. 2 and 3). Other comparisons can be made by using Table 4, Fig. 1 and the theoretical graphs provided in this report.

CONCLUSIONS AND FINAL REMARKS

One of the most important conclusions that can be drawn from the data presented here is that of the effect of thoron daughters on dosimeter reading. As has been shown this effect increases with decreasing WL(Rn)/WL(Tn) for a given radon daughter activity, thereby increasing the value of K_f (see Table 7), leading to an overestimation of the radon daughter dose exposure. As the biological effects of thoron daughters are not known and dose exposure limits have not as yet been set, it is important to determine the dose exposure contribution of both radon daughters and thoron daughters.

Based on the tests so far conducted it is suggested that a better, more reliable, pump be installed capable of giving a more constant flow over extended periods of time with a minimum of maintenance. Also, a switch to turn the pump off at any desired time, without erasing the data, would be a distinct advantage for calibration purposes as this additional feature would enable the dosimeter sampling time to be accurately determined. Moreover,

a 'softer' rim where the filter sits would considerably reduce the risk of filter tearing around the rim, thereby allowing air to flow freely around it instead of through the filter. Finally, dosimeter reading and data storage would be greatly facilitated by adding automatic printing facilities to the reader. It is our understanding that the latter is an already existing feature that α-NUCLEAR has recently added to its new dosimeter readers. Furthermore, we have been informed that α-NUCLEAR is at present completing the design of a more efficient and reliable pump for the dosimeter which should be ready for underground testing in the very near future. Further underground testing of the new dosimeter prototype and reader are planned by CANMET as soon as they become available.

ACKNOWLEDGEMENTS

We would like to express our appreciation to G.M. Denham (Manager, Alpha-NUCLEAR) for giving us the opportunity to conduct a technical evaluation of the α-NUCLEAR personal dosimeter. We would like to thank R. Shepherd (Alpha-NUCLEAR) for helpful discussions pertaining to the subject of this report. We are most appreciative to I. Montgomery (Rio Algom) for making the necessary arrangements to conduct this research. The authors are also grateful to R. Kowalchuk for his assistance in choosing the work site.

REFERENCES

1. McCurdy, D.E. "Thermoluminescent dosimetry for monitoring of uranium mines"; USAEC Report C00-1500-16; Colorado State University, Fort Collins, Colorado; June 1969.

2. McCurdy, D.E., Schiager, K.J. and Flack, E.D. "Thermoluminescent dosimetry for personal monitoring of uranium miners"; Health Physics, vol 17, p 414; 1969.

3. White, O. Jr. "An evaluation of six radon dosimeters"; USAEC Health and Safety Laboratory Technical Memorandum 69-23; Oct. 1969. "Evaluation of MIT and ORNL radon daughter dosimeters"; USAEC Health and Safety Laboratory Technical Memorandum 70-3; July 1970. "Evaluation of MOD and ORNL radon daughter dosimeters"; USAEC Health and Safety Laboratory Technical Memorandum 71-17; Oct 1971.

4. Rock, L.R. "Measurement of employee's individual cumulative exposures to radon daughters as practiced in the United States"; Personal Dosimetry and Area Monitoring Suitable for Radon and Daughter Products; Proc of the NEA Special Meeting, Elliot Lake, Ontario, Canada; pp 71-90; 1976.

5. Breslin, A.J. "MOD working level dosimeter"; Personal Dosimetry and Area Monitoring Suitable for Radon and Daughter Products"; Proc of the NEA Special Meeting, Elliot Lake, Ontario, Canada; pp 91-100; 1976.

6. Chapuis, A.M., See for instance "Dosimetry in French uranium mines"; Presented at a meeting on Personal Dosimetry and Personal Exposure Estimation, Ottawa, Ontario, Oct 5th 1978, sponsored by AECB.

7. Durkin, J. "An electronic instrument for radon daughter dosimetry"; Report of Investigation 8255, U.S. Bureau of Mines, 1977. See also Health Physics vol 37, pp 757-764, 1979.

8. The present prototype (α-NUCLEAR).

9. Kusnetz, H.L. "Radon daughters in mine atmospheres"; Am Ind Hyg Assoc J, vol 17, p 1; 1956.

10. Ibid "Radon daughters in mine atmospheres - a field method for determining concentrations"; Ind Hyg Quarterly; March 1956.

11. Thomas, J.W. "Measurement of radon daughters in air"; Health Physics, vol 23, pp 783-789; 1972.

12. Markov, K.P., Ryabov, N.V. and Stas, K.N. "A rapid method for estimating the hazard associated with the presence of radon daughter products in air"; At Ehnerg, vol 12, p 315; 1962.

13. Rolle, R. "Improved radon daughter monitoring procedure"; Am Ind Hyg Assoc J, pp 153-160; March/April, 1969.

14. Rolle, R. "Radon daughters and age of ventilation air"; Health Physics, vol 23, pp 118-120; 1972.

15. Droullard, R.F. and Holub, R.F. "Continuous working level measurements using alpha or beta detectors"; Report of Investigation RI 8237; US Bureau of Mines; 1977.

16. Holub, R.F. and Droullard, R.F. "Evaluation of various radon daughter measurement methods"; Proc. Workshop on Methods for Measuring Radiation in and Around Uranium Mills, Albuquerque, New Mexico, May 23-26, 1977; E.D. Harvard (Ed), vol 3, no. 9, pp 197-219; 1977.

17. Ibid "Radon daughter mixture distributions in uranium mine atmospheres"; Technical Report RI 8316; U.S. Bureau of Mines; 1978.

18. Evans, R.D. "Engineers' guide to the elementary behaviour of radon daughters"; Health Physics, vol 17, pp 229-252; 1969.

19. Bigu, J. Report in preparation.

20. Bigu, J. Report in preparation.

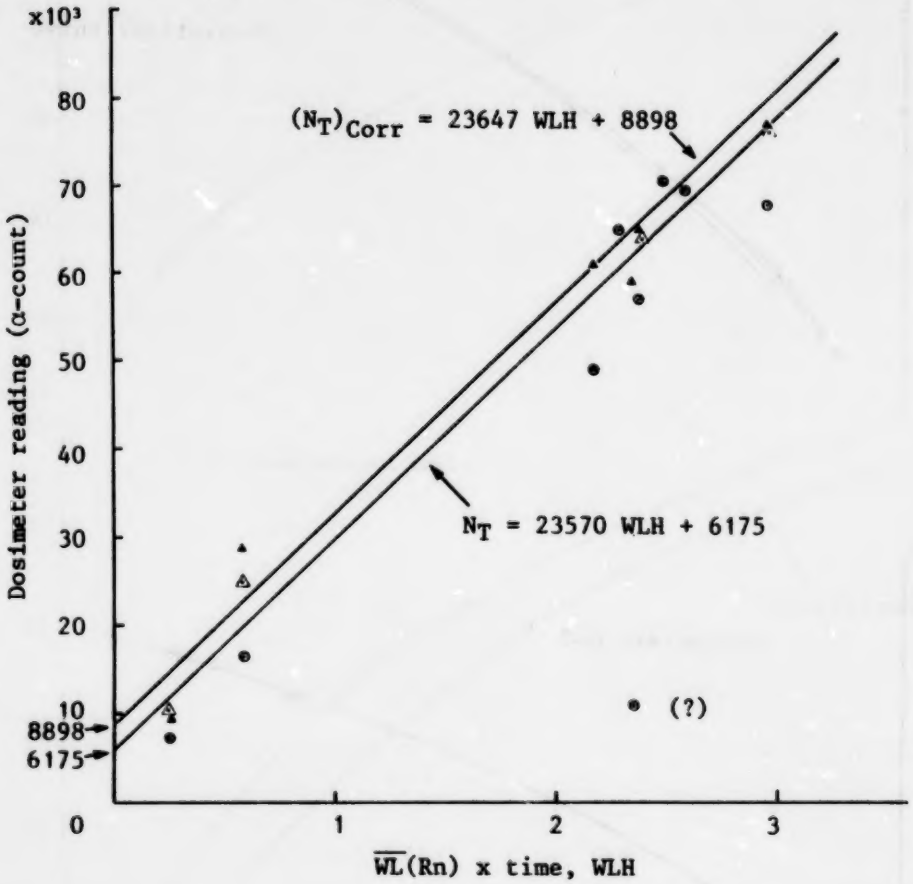

Fig. 1: Dosimeter reading (α-count) versus $\overline{WL}$(Rn) x t for two dosimeters: α-1 (▲) and α-2 (●). Upper curve represents 'normalized' (to Q = 0.1 L/min) values. Lower curve represents uncorrected values. Triangles indicate corrected values of α-2. α-1 required little correction and the latter is not shown in the graph. Curves are best fitted lines through all data points.

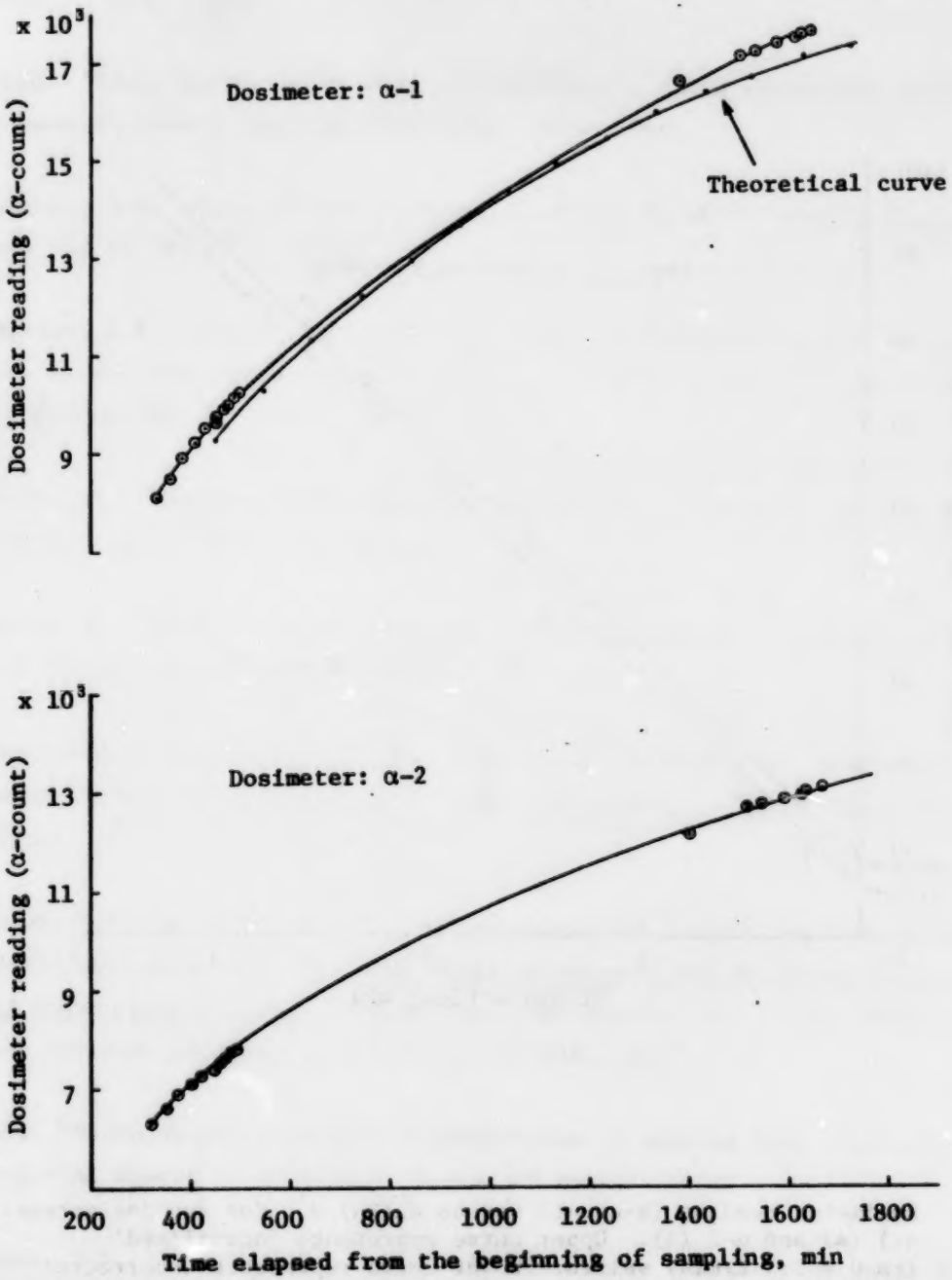

Fig. 2: Dosimeter reading versus time elapsed from the beginning of sampling. Upper and lower curves (•) correspond, respectively, to experimental data pertaining to dosimeters α-1 and α-2. The curve through the dots represents the theoretically calculated values for α-1. Data taken December 4th, 1979.

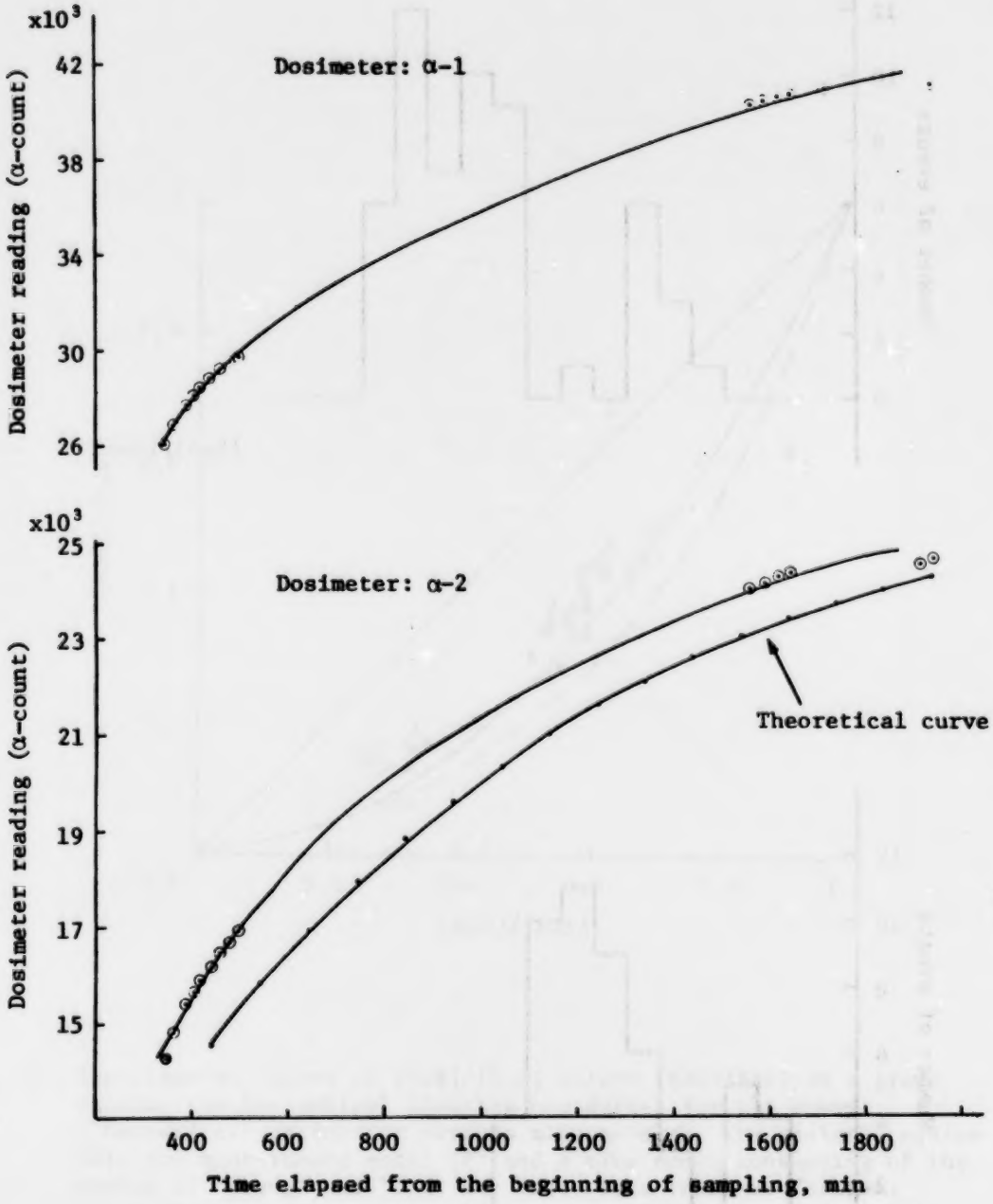

Fig. 3: Dosimeter reading versus time elapsed from the beginning of sampling. Upper and lower curves (⊙) correspond, respectively, to experimental data pertaining to dosimeters α-1 and α-2. The curve through the dots represents the theoretically calculated values for α-1. Data taken on December 7th, 1979.

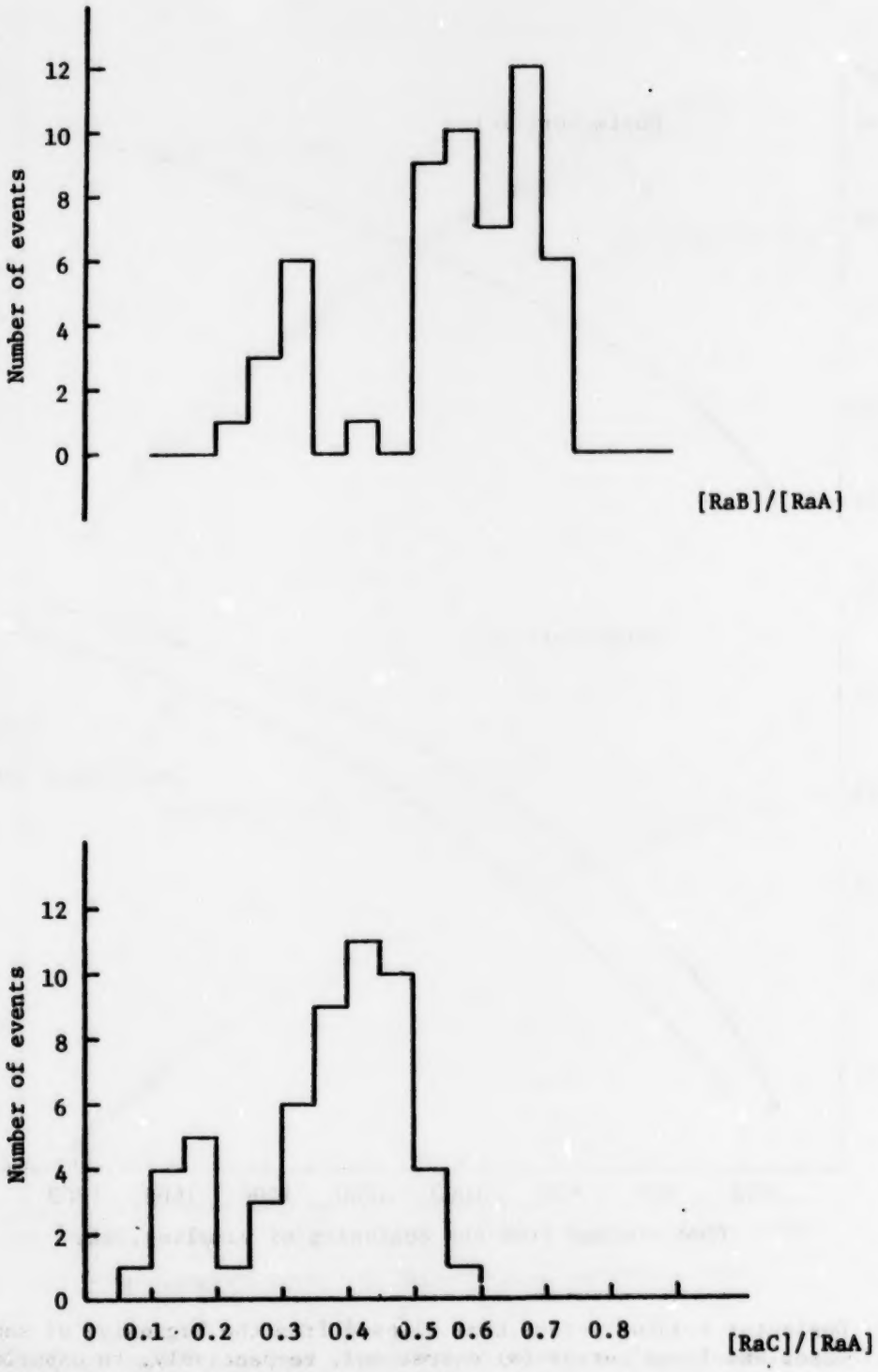

Fig. 4: Number of occurrences of the ratios [RaB]/[RaA] and [RaC]/[RaA] from the field data.

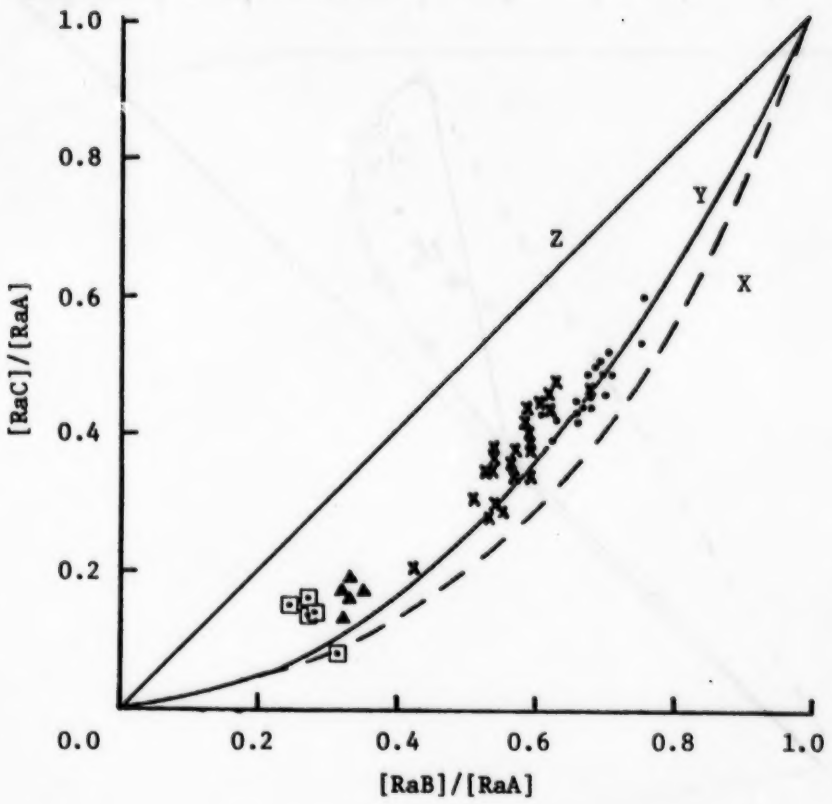

Fig. 5: Experimental values of [RaB]/[RaA] versus [RaC]/RaA] on a graph showing the theoretical limiting boundaries for the above (theoretical) ratios for various mine models: the isolated system (X), the mine-tunnel model (Y) and a mine model consisting of the mixing of 'young' and 'old' air (Z). Data taken as follows: Slusher's bend (⊡); garage (•); stope with high air flow (▲); and stope with low air flow (X).

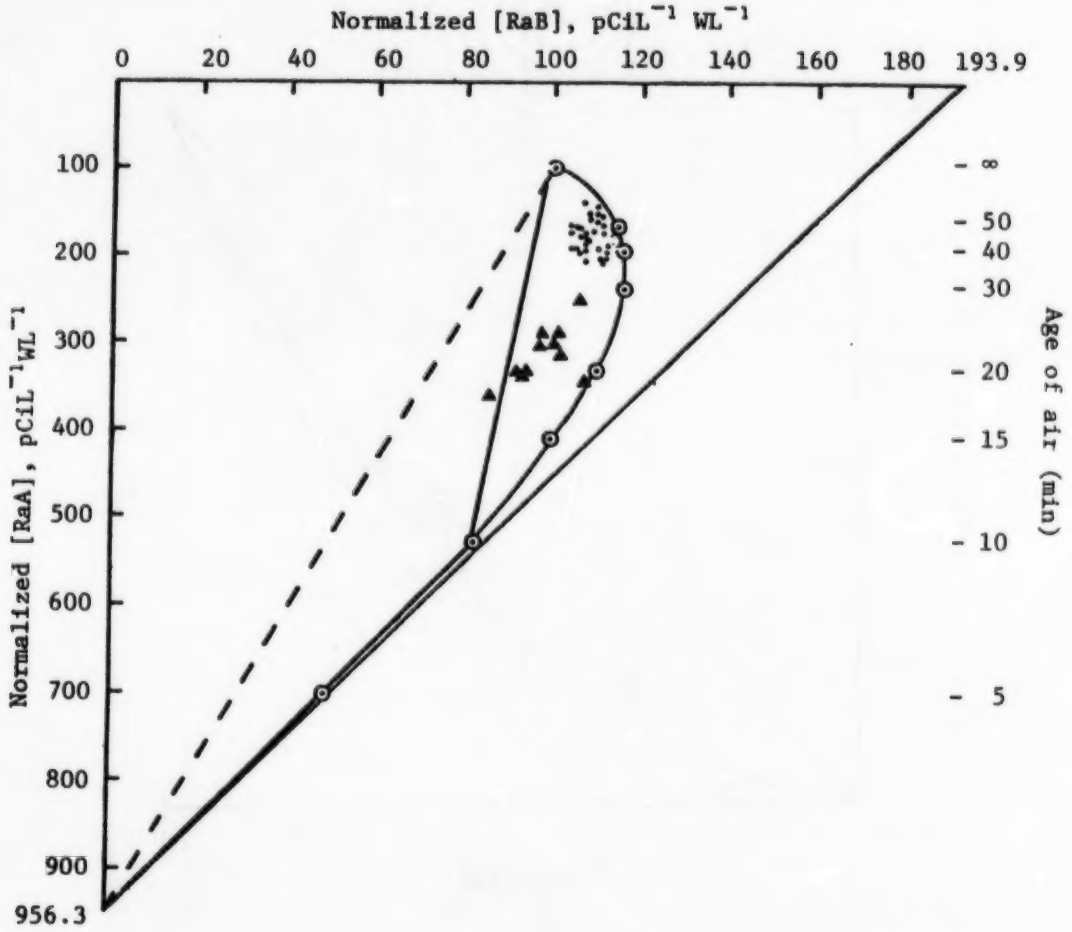

Fig. 6: Experimental normalized (relative to WL(Rn)) values of [RaA] and [RaB]. Dots and full triangles indicate, respectively, data taken in low and high air flow areas.

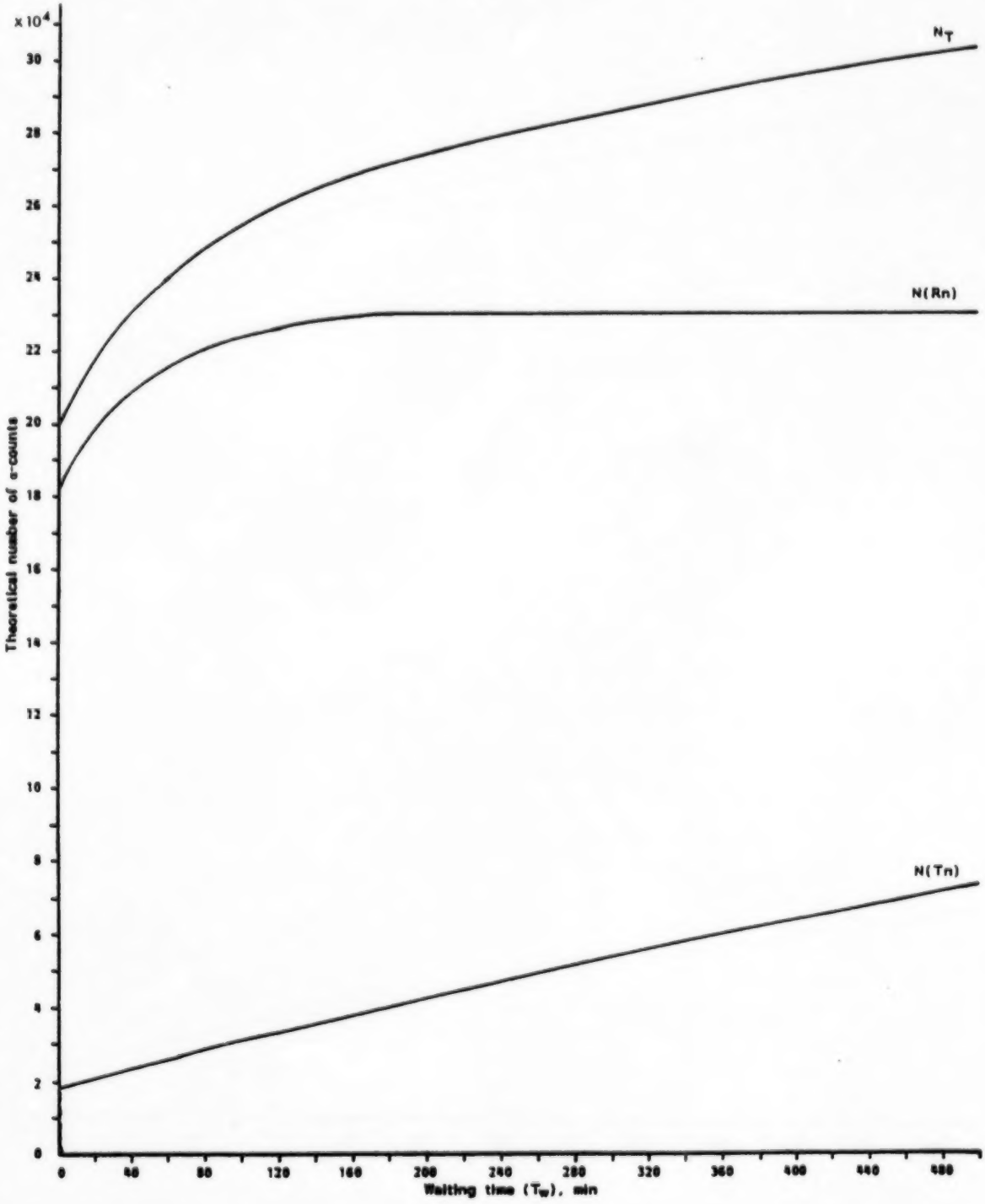

Fig. 7 - Theoretical number of α-counts due to radon daughters (N(Rn)), thoron daughters (N(Tn)) and total N_T as a function of waiting time (T_W) for a sampling time (T_S) of 240 min. Data have been normalized to $\varepsilon = 1.0$ and $Q = 0.1$ L/min. Calculations have been done for a radon daughter disequilibrium ratio of 1:0.68:0.47 where [RaA] = 89.58 pCi/L and [ThB] = 2.87 pCi/L, i.e., garage.

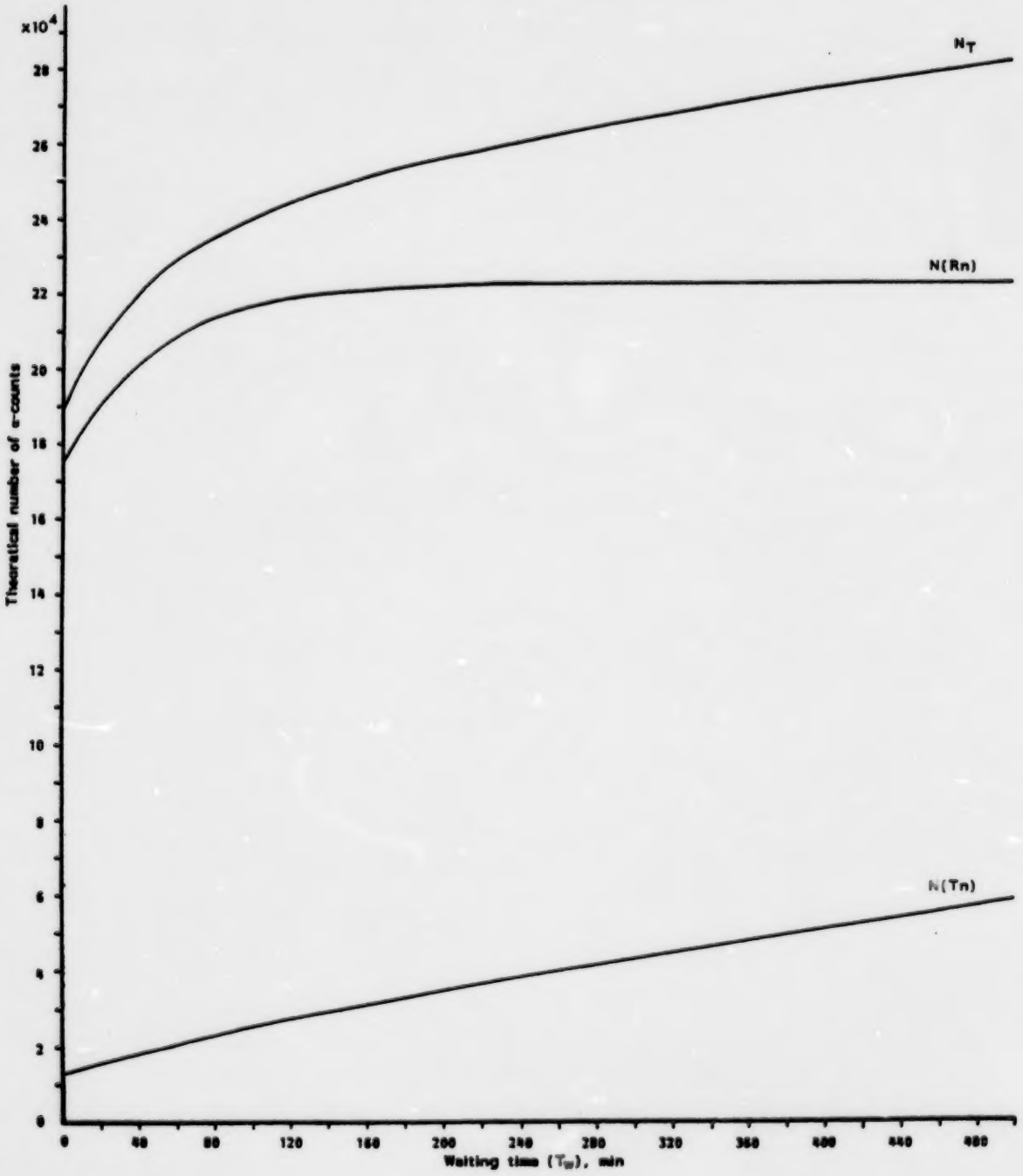

Fig. 8 - Theoretical number of α-counts due to radon daughters (N(Rn)), thoron daughters (N(Tn)) and total N_T as a function of waiting time (T_W) for sampling time (T_S) of 240 min. Data have been normalized to ϵ = 1.0 and Q = 0.1 L/min. Calculations have been done for a radon daughter disequilibrium ratio of 1:0.57:0.37 where [RaA] = 100.84 pCi/L, and [ThB] = 2.30 pCi/L, i.e., working stope with low air flow.

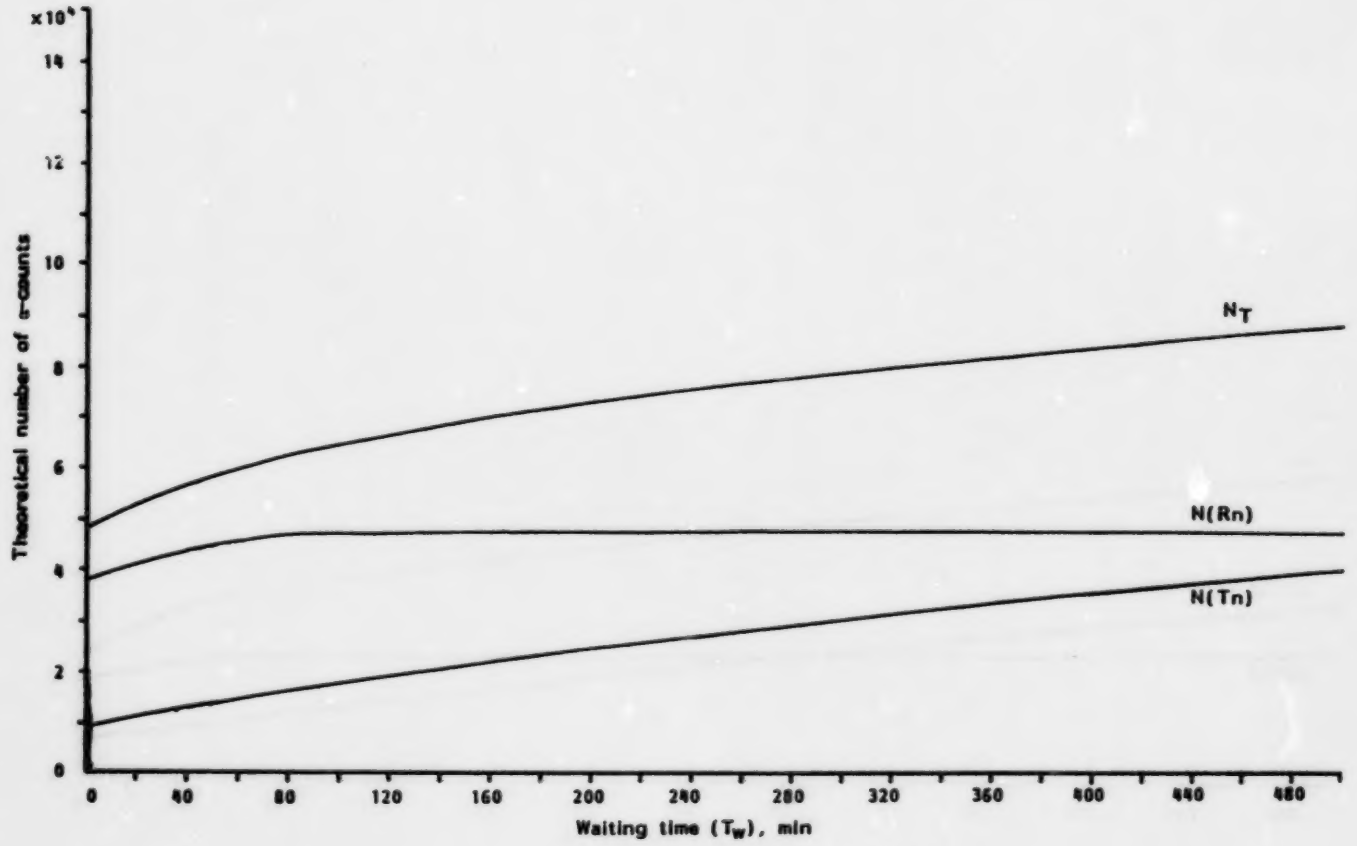

Fig. 9 - Theoretical number of α-counts due to radon daughters (N(Rn)), thoron daughters (N(Tn)) and total N_T as a function of waiting time (T_w) for a sampling time (T_s) of 240 min. Data have been normalized to ε = 1.0 and Q = 0.1 L/min. Calculations have been done for a radon daughter disequilibrium ratio of 1:0.3:0.15 where [RaA] = 36.72 pCi/L and [ThB] = 1.59 pCi/L, working stope with high air flow .

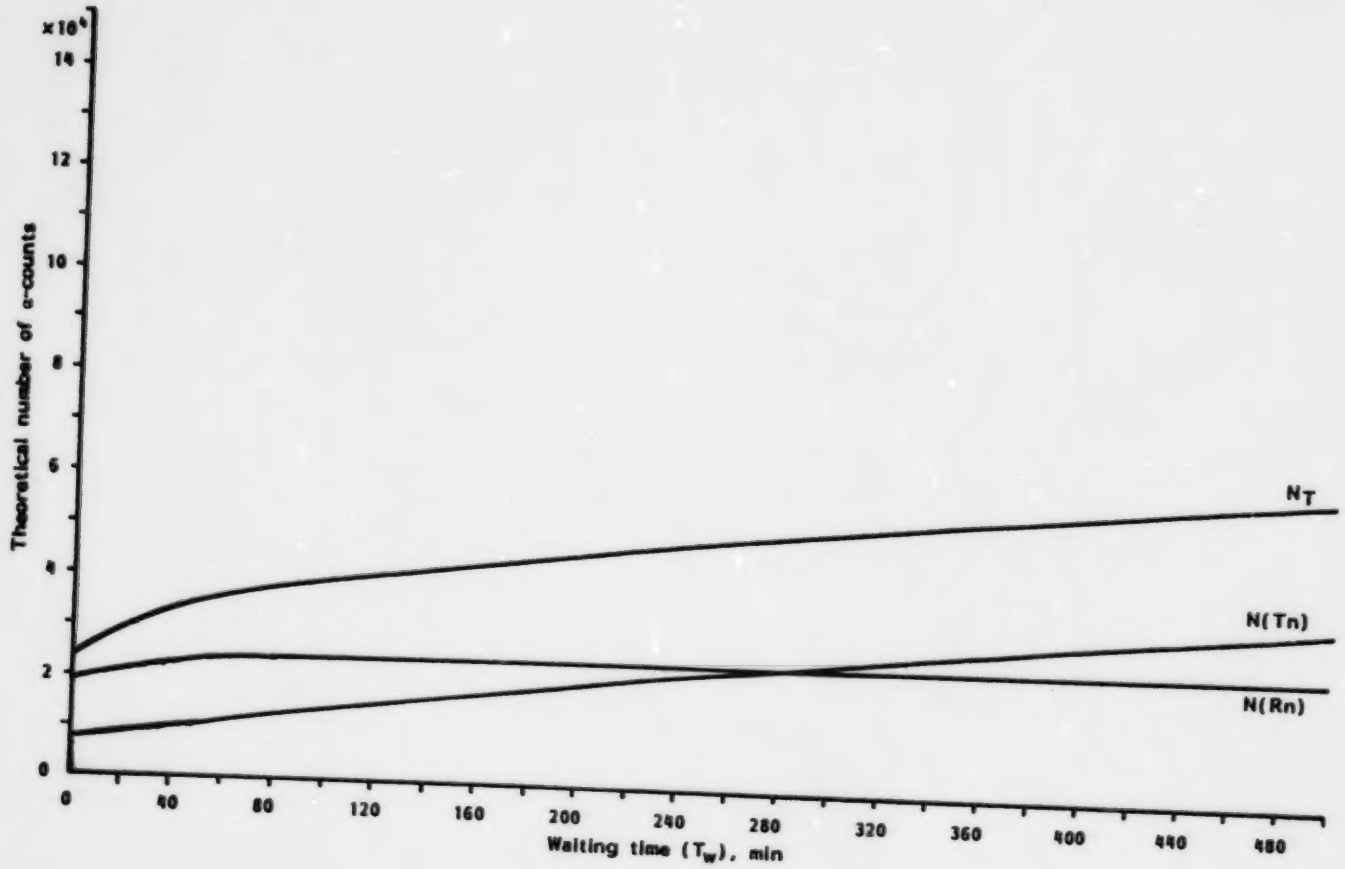

Fig. 10 - Theoretical number of α-counts due to radon daughters (N(Rn)), thoron daughters (N(Tn)) and total N_T as a function of waiting time (T_w) for a sampling time (T_s) of 240 min. Data have been normalized to ε = 1.0 and Q = 0.1 L/min. Calculations have been done for a radon daughter disequilibrium ratio of 1:0.3:0.15 where [RaA] = 19.05 pCi/L and [ThB] = 1.36 pCi/L, i.e., slusher's bench.

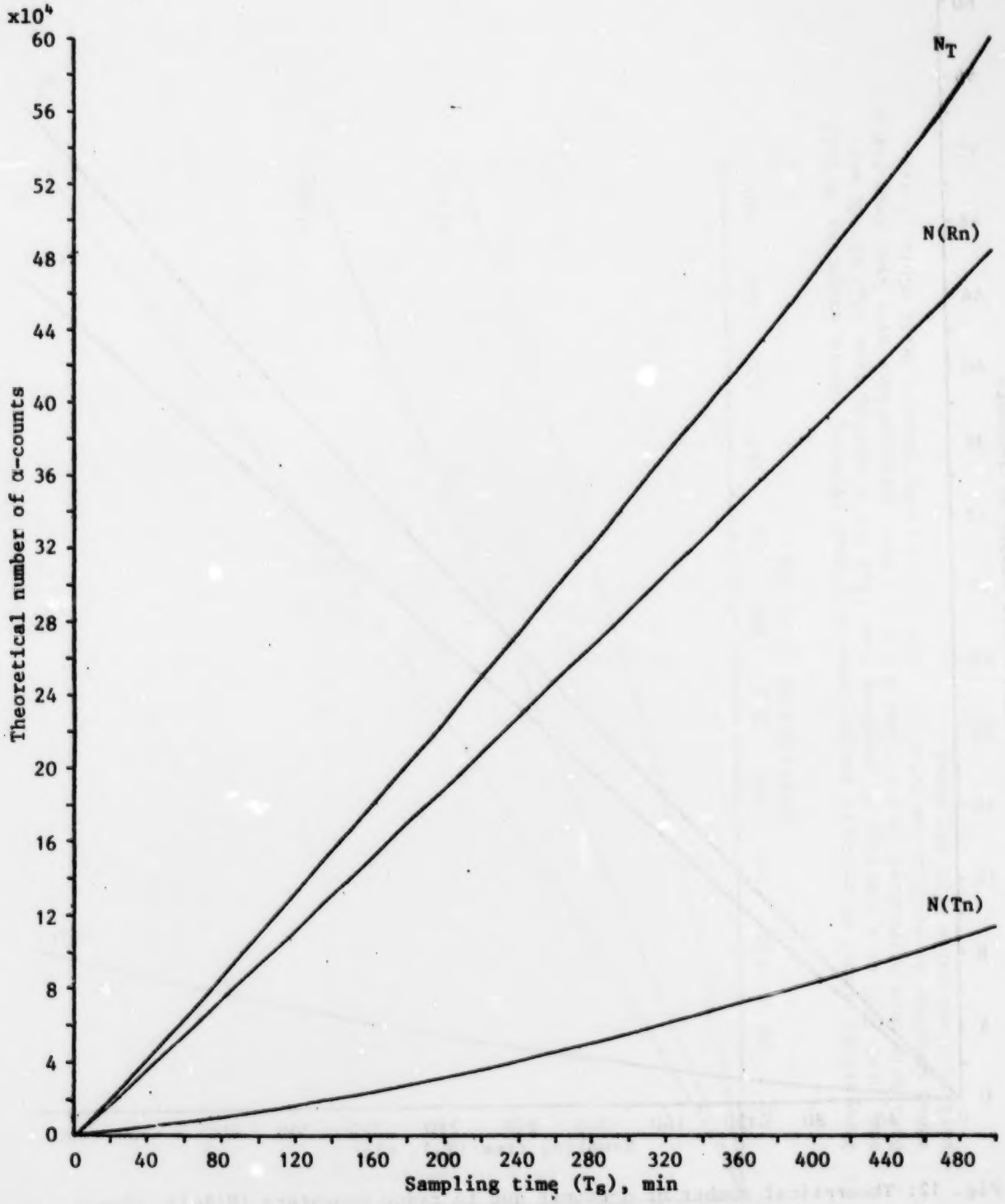

Fig. 11: Theoretical number of α-counts due to radon daughters (N(Rn)), thoron daughters (N(Tn)) and total (N_T) as a function of sampling time (T_S) for a waiting time (T_W) of 180 min. Data have been normalized to $\varepsilon = 1$ and $Q = 0.1$ L/min. Calculations have been done for a radon daughter disequilibrium ratio of: 1:0.68:0.47 where [RaA] = 89.58 pCi/L, i.e., garage.

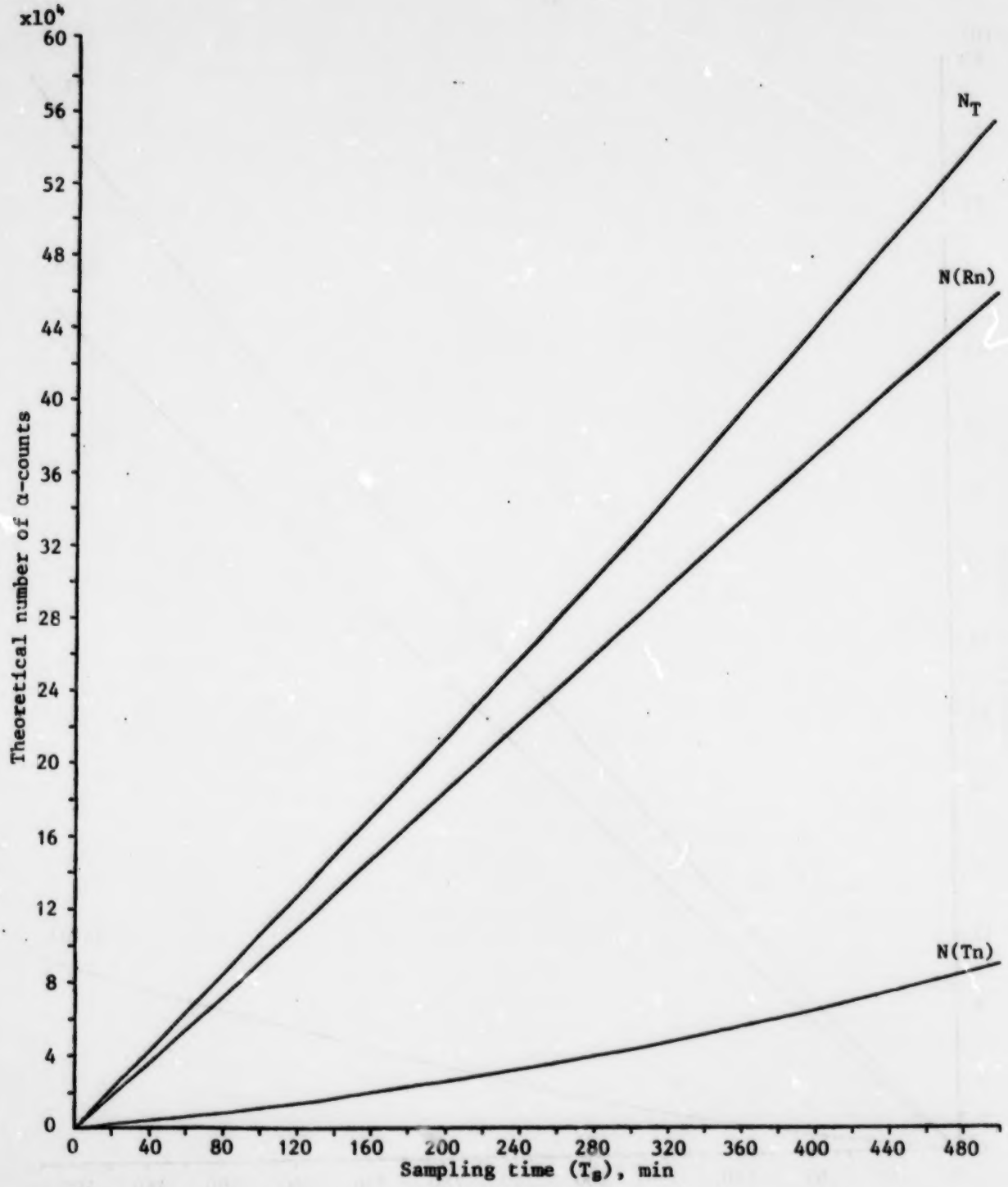

Fig. 12: Theoretical number of α-counts due to radon daughters (N(Rn)), thoron daughters (N(Tn)) and total (N_T) as a function of sampling time (T_s) for a waiting time (T_w) of 180 min. Data have been normalized to $\varepsilon = 1$ and $Q = 0.1$ L/min. Calculations have been done for a radon daughter disequilibrium ratio of: 1:0.57:0.37 where [RaA] = 100.84 pCi/L, i.e., working stope (with low air flow).

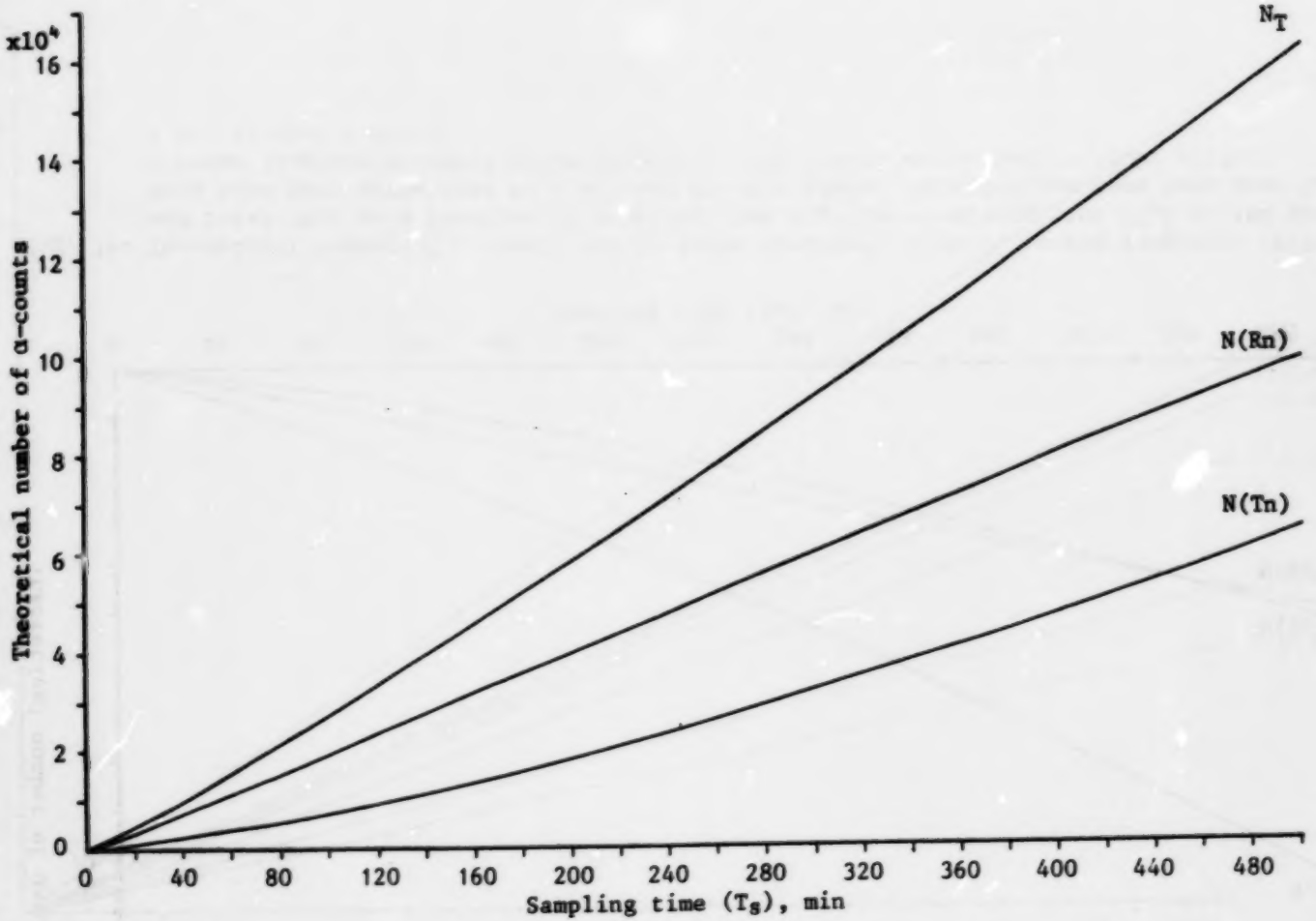

Fig. 13: Theoretical number of α-counts due to radon daughters (N(Rn)), thoron daughters (N(Tn)) and total (N_T) as a function of sampling time (T_s) for a waiting time (T_w) of 180 min. Data have been normalized to $\varepsilon = 1$ and $Q = 0.1$ L/min. Calculations have been done for a radon daughter disequilibrium ratio of: 1:0.3:0.15 where [RaA] = 36.72 pCi/L, i.e., working stope (with high air flow).

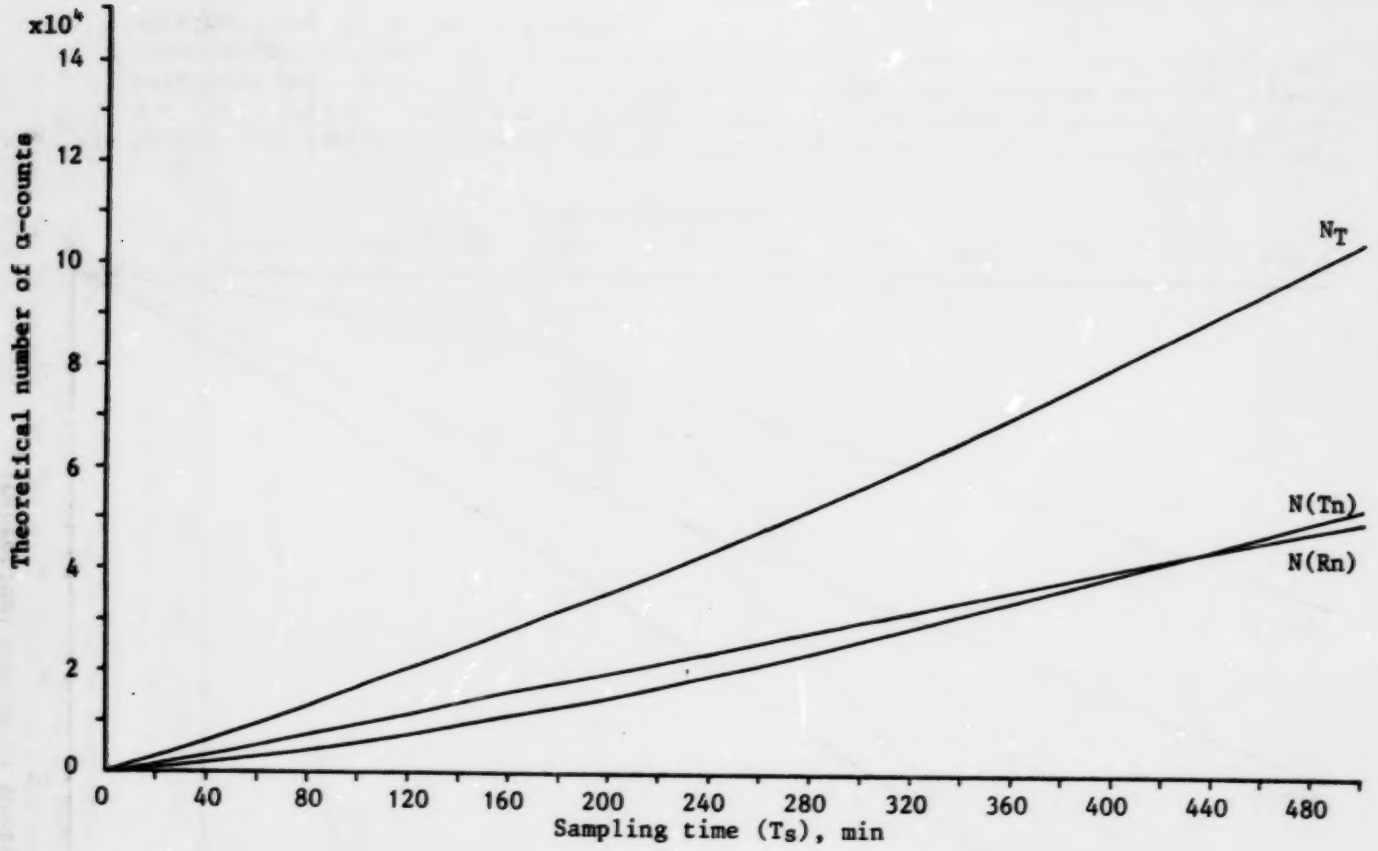

Fig. 14: Theoretical number of α-counts due to radon daughters (N(Rn)), thoron daughters (N(Tn)) and total (N_T) as a function of sampling time (T_s) for a waiting time (T_w) of 180 min. Data have been normalized to $\varepsilon = 1$ and $Q = 0.1$ L/min. Calculations have been done for a radon daughter disequilibrium ratio of: 1:0.3:0.15 where [RaA] = 19.05 pCi/L, i.e., slusher's bench.

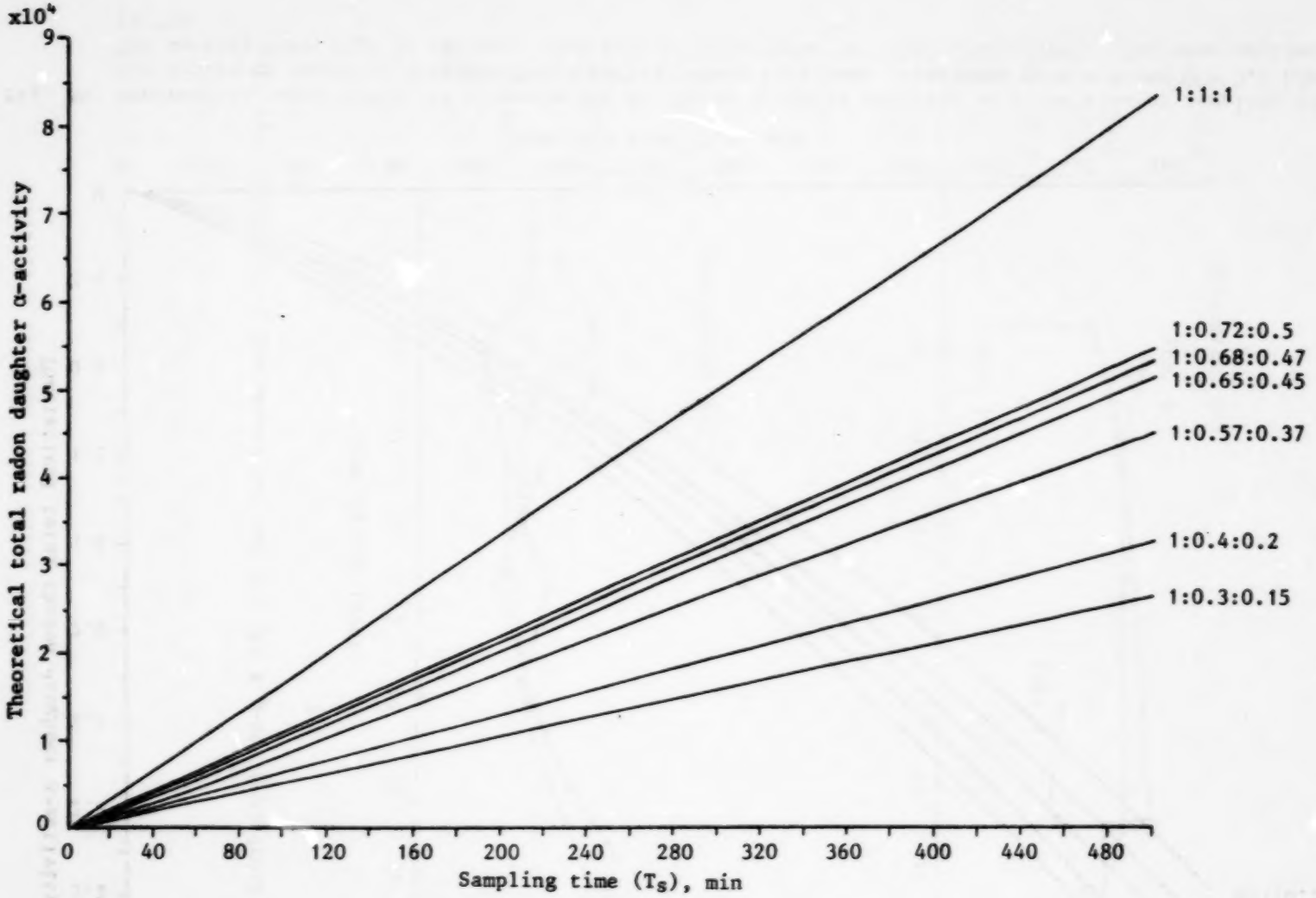

Fig. 15: Theoretical total number of α-counts due to radon daughter activity as a function of sampling time for different daughter disequilibrium ratios. Data have been normalized to $\varepsilon = 1$ and $Q = 0.1$ L/min. The waiting time (T_W) is 180 min.

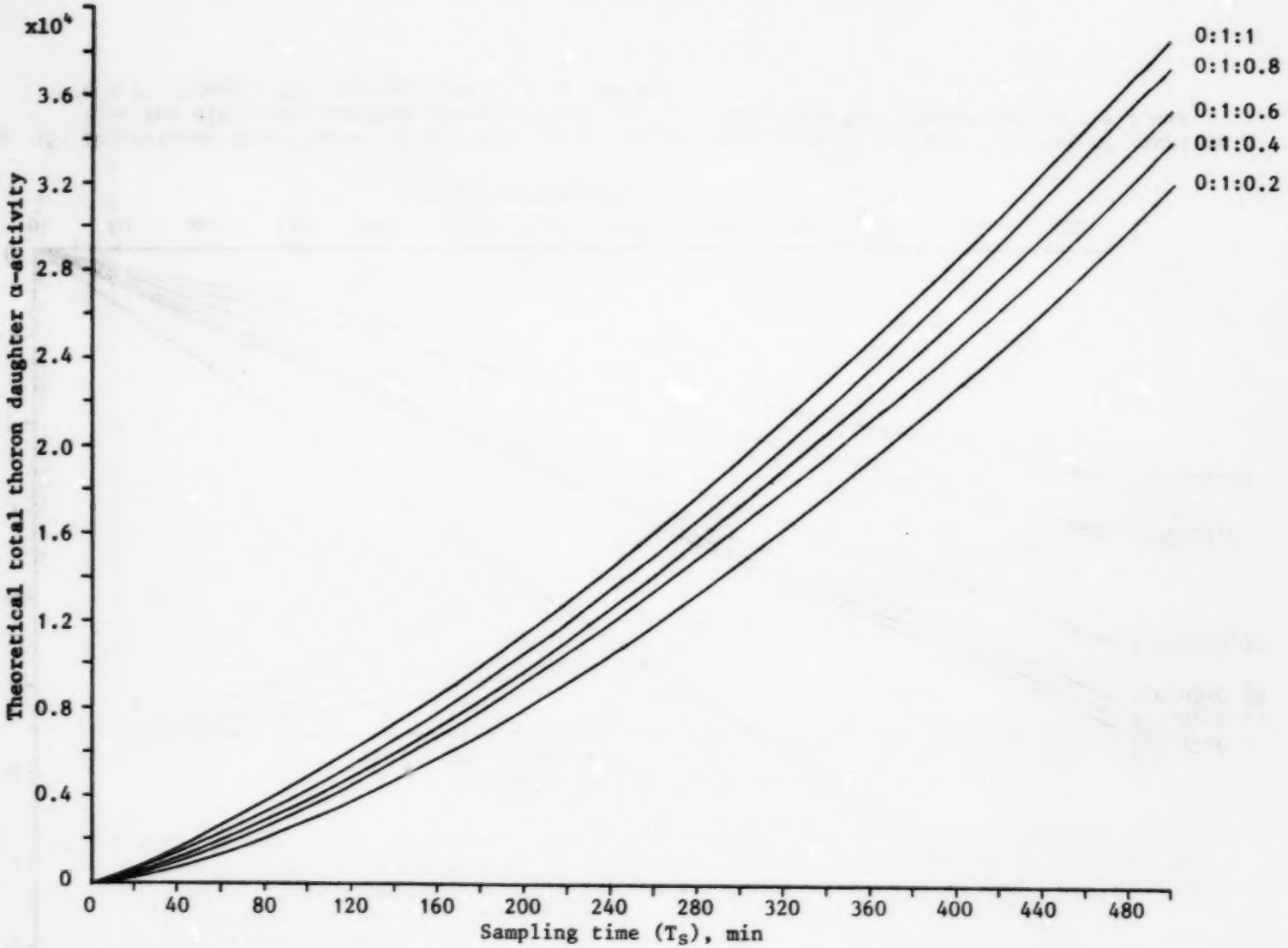

Fig. 16: Theoretical total number of α-counts due to thoron daughter activity as a function of sampling time for different daughter disequilibrium ratios. Data have been normalized to ε = 1 and Q = 0.1 L/min. The waiting time (T_W) is 180 min. The ratios above refer to [ThA]:[ThB]:[ThC]. The same applies to Fig. 17.

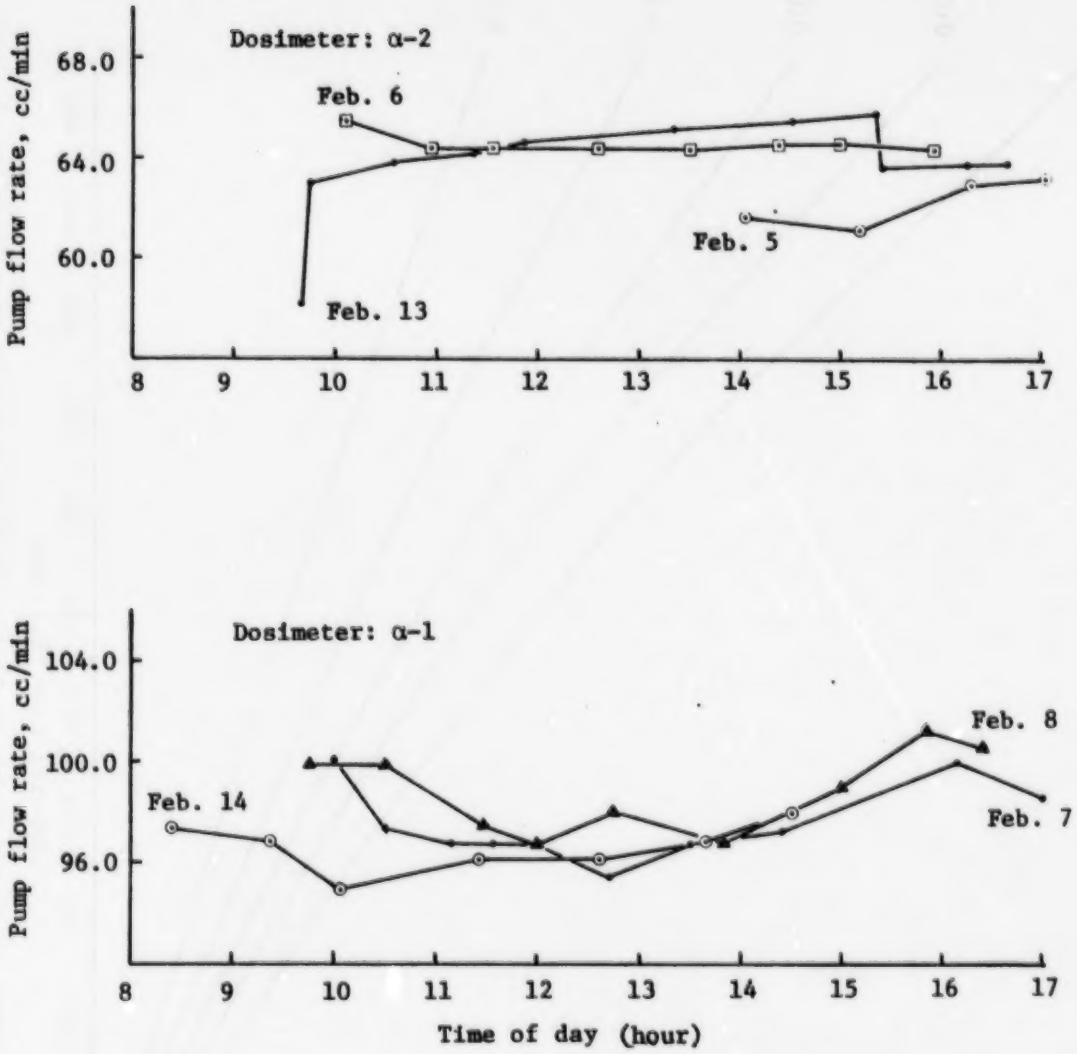

Fig. 18: Flow rate of dosimeters α-1 and α-2 for a 3-day laboratory test.

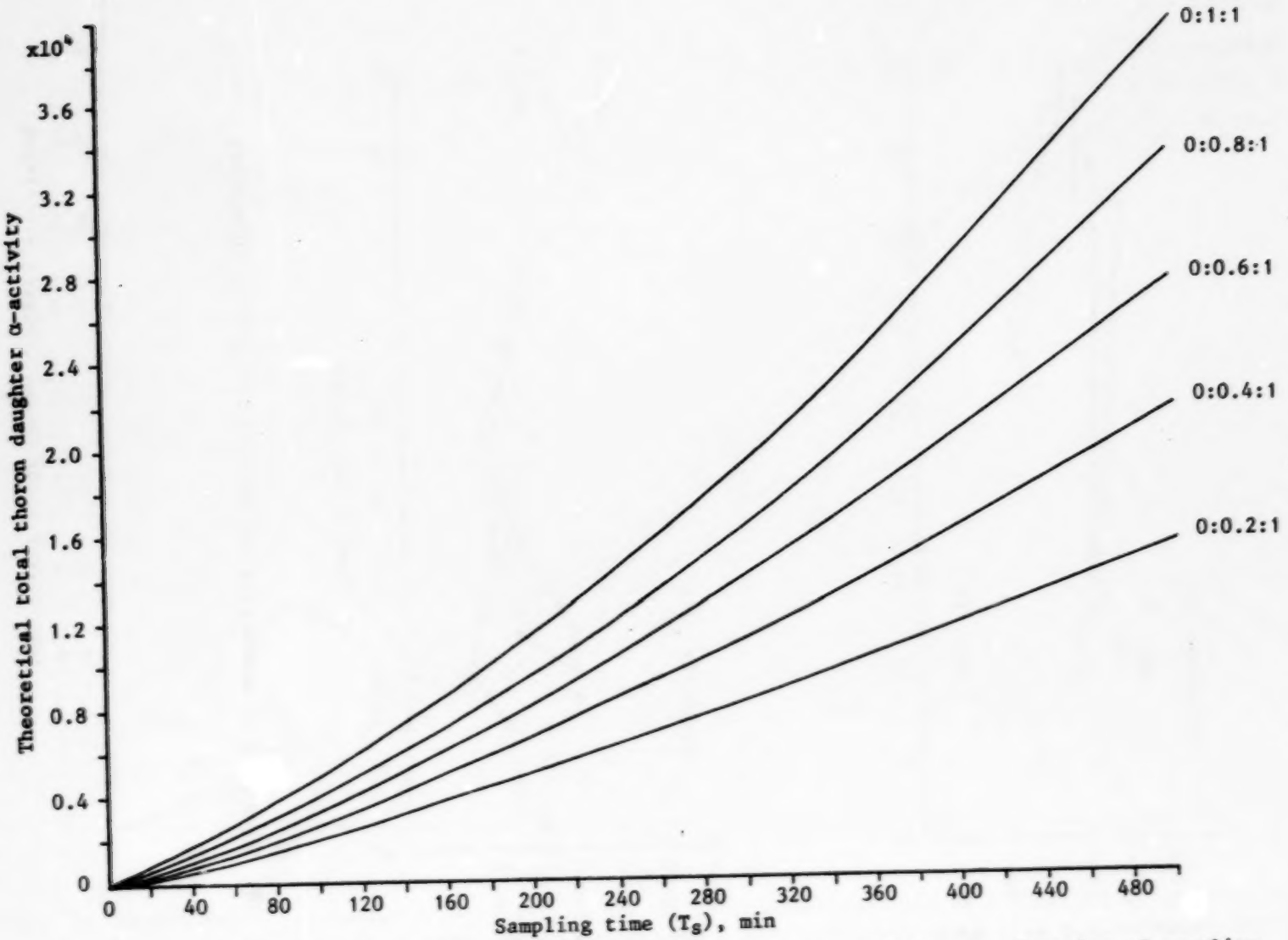

Fig. 17: Theoretical total number of α-counts due to thoron daughter activity as a function of sampling time for different daughter disequilibrium ratios. Data have been normalized to $\varepsilon = 1$ and $Q = 0.1$ L/min. The waiting time (T_w) is 180 min.